THEORY

EXPOSURE MODEL

DATE: December 2023

The EXPS model calculates (a) whether an observer is engulfed by a flame; and (b) geometric view factor for an observer exposed to that flame. It also provides the facility to maximise the view factor by varying observer orientation.

No.	Date	Reason for Issue	Prepared by	Verified by	Approved by
1	Sept 2001	PHAST 6.1	Mike Harper	Henk Witlox	
2	Feb 2003	SAFETI 6.3	Mike Harper		
3	June 2003	SAFETI 6.4	Mike Harper	Henk Witlox	
4	May 2021	Apply new template	D. Vatier		
5	October 2021	Updates for 8.6 – multi-point source emitter modelling	D. Worthington and A.O.Oke	D. Worthington	

Date: December 2023

Prepared by: Digital Solutions at DNV

ABSTRACT

The exposure model calculates the view factor for an observer exposed to a flame. The general theory for view factor determination is described, and is followed by specific theory developed for a number of different flame surface geometries. A separate model for testing whether observers are engulfed by different flame geometries is also presented. A summary of model verification is included, as are a number of potential future revisions of the model. Two appendices describe the derivation of view factors for a plane, and a method to find the minimum distance between observer and flame.

Table of contents

Table of figures

1 INTRODUCTION

The radiation received by an observer exposed to a flame is directly proportional to both the flame surface emissive power (SEP) and the geometric view factor (V) of the observer. While SEP is either user-specified or calculated by the fire models, V is calculated by the exposure model, EXPS, which is used in all radiation based calculations in PHAST and SAFETI. This report is primarily concerned with establishing the theory of these view factor calculations. Several similar models are developed for particular flame surface geometries, and the method of solution for each of these models described.

The view factor calculation is only meaningful for observers outside the flame. Therefore a separate model in EXPS allows determination of whether or not this is the case. Typically this is tested first by users to allow special handling or assignment of arbitrary values (*e.g.* V = 1, lethality = 100% in PHAST) for engulfed observers.

The structure of the report is as follows. Firstly the general theory and definitions relevant to all the view factor models are presented in Section 2. In Section 3 the flame geometry is discussed, before the view factor models for particular flame surface geometries are developed (Section 4). Next a separate section describes the method for testing engulfed observers for different flame geometries. Later sections describe model verification and future developments.

The model has been rewritten for PHAST 6.4, following earlier review work that had identified shortcomings in the old model.

2 GENERAL THEORY OF GEOMETRIC VIEW FACTORS

2.1 Incident Radiation and View Factors

Consider any flame surface S, with P a point on that surface. Radiation emitted from P is received by an observer, O, on a plane surface (
Figure 1). The radiation intensity, I (W/m^2), received by the observer is a product of the flame emissive power, E (W/m^2), and a dimensionless geometric view factor, V:

$$I = EV \qquad (1)$$

Typically view factor varies from zero (when the observer cannot 'see' the flame surface and receives no radiation) to one (when an observer receives radiation equivalent to the SEP of the flame).

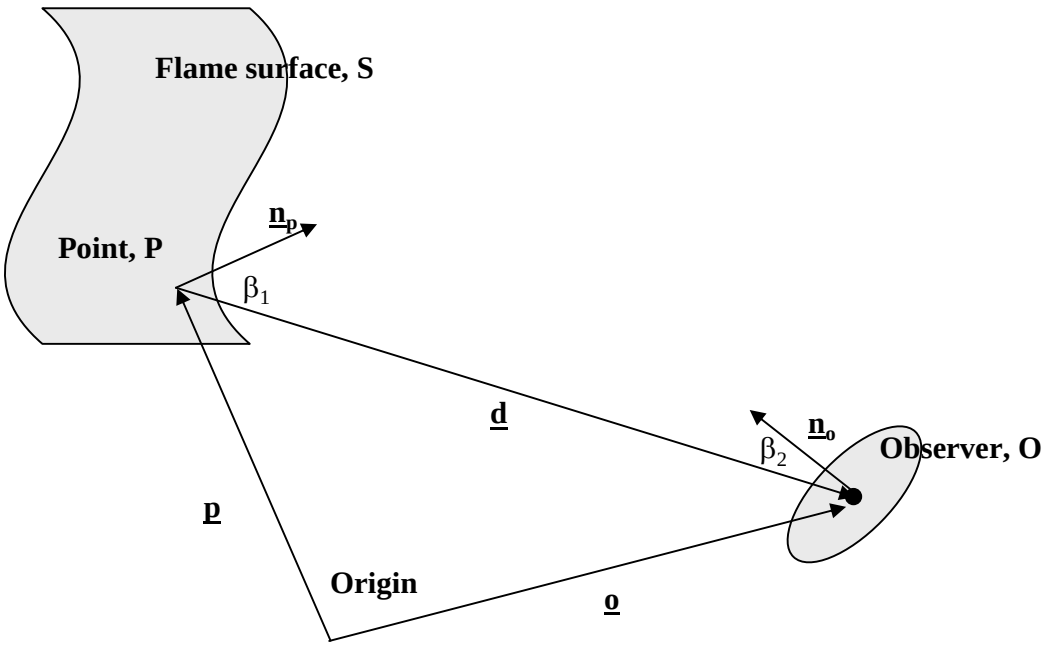

Figure 1. Definition of view factor.

The model for computing geometric view factor, V, for an observer O exposed to a flame surface, S, is (Cook *et al.*, 1989; Mudan, 1984):

$$V = \iint_S \frac{\tau \cos(\beta_1)\cos(\beta_2)}{\pi\ \mathrm{d}^2}\, dS \qquad (2)$$

$\underline{d}$ is the vector from the point P to the observer, O ($\underline{o} - \underline{p}$)
β_1 is the angle between the normal ($\underline{n}_p$) to the flame surface at P, and $\underline{d}$
β_2 is the angle between the observer plane normal ($\underline{n}_o$) and $-\underline{d}$
τ is the atmospheric transmissivity, the fraction of radiation not absorbed by the atmosphere

This can be more usefully expressed in terms of the unit normal vectors $\underline{n}_p$ and $\underline{n}_o$:

$$V = \frac{1}{\pi}\iint_S \frac{\tau\left(\underline{d}\cdot\underline{\mathrm{n}}_\mathrm{p}\right)\left(-\underline{d}\cdot\underline{n}_o\right)}{\mathrm{d}^4}\, dS \qquad (3)$$

In addition, the integrand is subject to a constraint that where either of the dot products is negative, then the overall value of the expression is zero. This constraint is necessary as whenever flame segments are 'behind' the observer plane, or observers 'behind' the flame surface, there is no contribution from that point to the view factor:

$$V = \frac{1}{\pi}\iint_S \frac{\tau\ \max\left(\underline{d}\cdot\underline{\mathrm{n}}_\mathrm{p},0\right)\max\left(-\underline{d}\cdot\underline{n}_o,0\right)}{\mathrm{d}^4}\, dS \qquad (4)$$

By definition, the parametric values for the integral limits must therefore satisfy the conditions:

$$\min\left(\underline{n}_p\cdot\underline{d}, \underline{n}_o\cdot -\underline{d}\right) = 0 \qquad (5)$$

However, only the first dot product is used in estimating integral limits[1]:

$$\underline{n}_p\cdot\underline{d} = 0 \qquad (6)$$

Although analytical solutions exist for certain simple flame shapes[2] (Mudan, 1984), the view factor is normally calculated by evaluating the integral of this Equation numerically over the entire flame surface. This is most frequently done in EXPS by deriving an expression for the integrand in terms of the two parameters defining the surface S.

The flame and surface are described within a 3D Cartesian co-ordinate system (X,Y,Z). X is distance downwind of the flame, Y is distance crosswind, and Z vertical height above the ground. Note that some specific flame geometry models use a local 2D or 3D system for simplicity, always denoted by lower case symbols (x,y,z).

[1] The other dot product can still be negative, but this is handled by setting the value of the integrand to zero. This proved more efficient computationally. This is especially the case when one considers that normally these models are used in 'optimized' mode, where observers point towards the flame and the dot product will normally be positive.

[2] Usually requiring the additional assumption that τ = constant.

1.1 Incident Radiation and Multiple Point Approach

Consider a flame represented by its centreline.

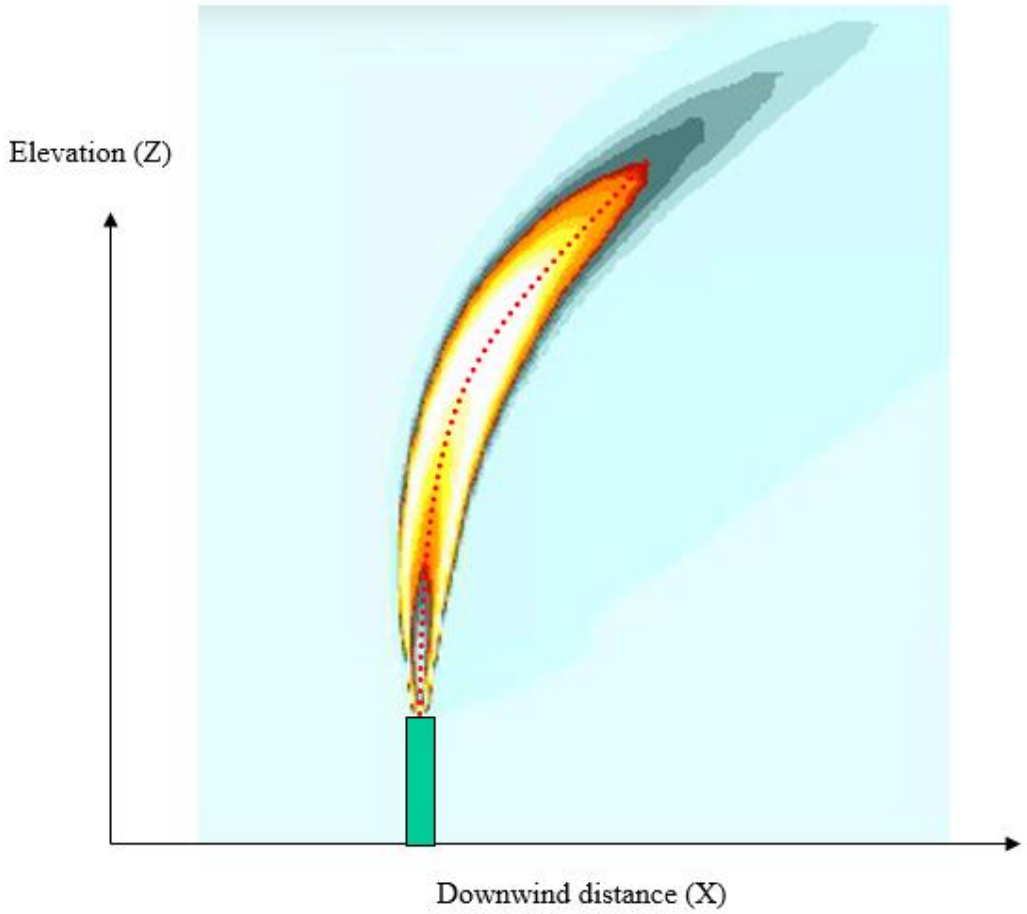

Instead of having a solid surface where the flame has a variable width along its length it has the concept of a weighting factor *f(l)* representing the proportion of energy being emitted at different positions along the flame length.

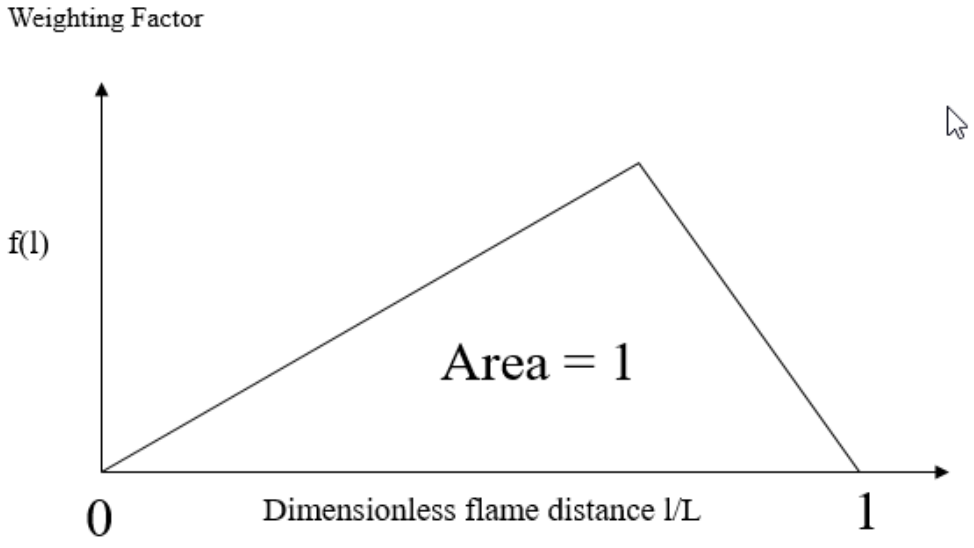

The radiation intensity, I (W/m^2), received by the observer is a product of the flame emissive power, P (W), and an effective geometric intensity I' with the dimensions ($/m^2$).

I=PI' **(7)**

Consider a flame centreline with an overall length of L, with P a point on that line. Radiation emitted from P is received by an observer, O.

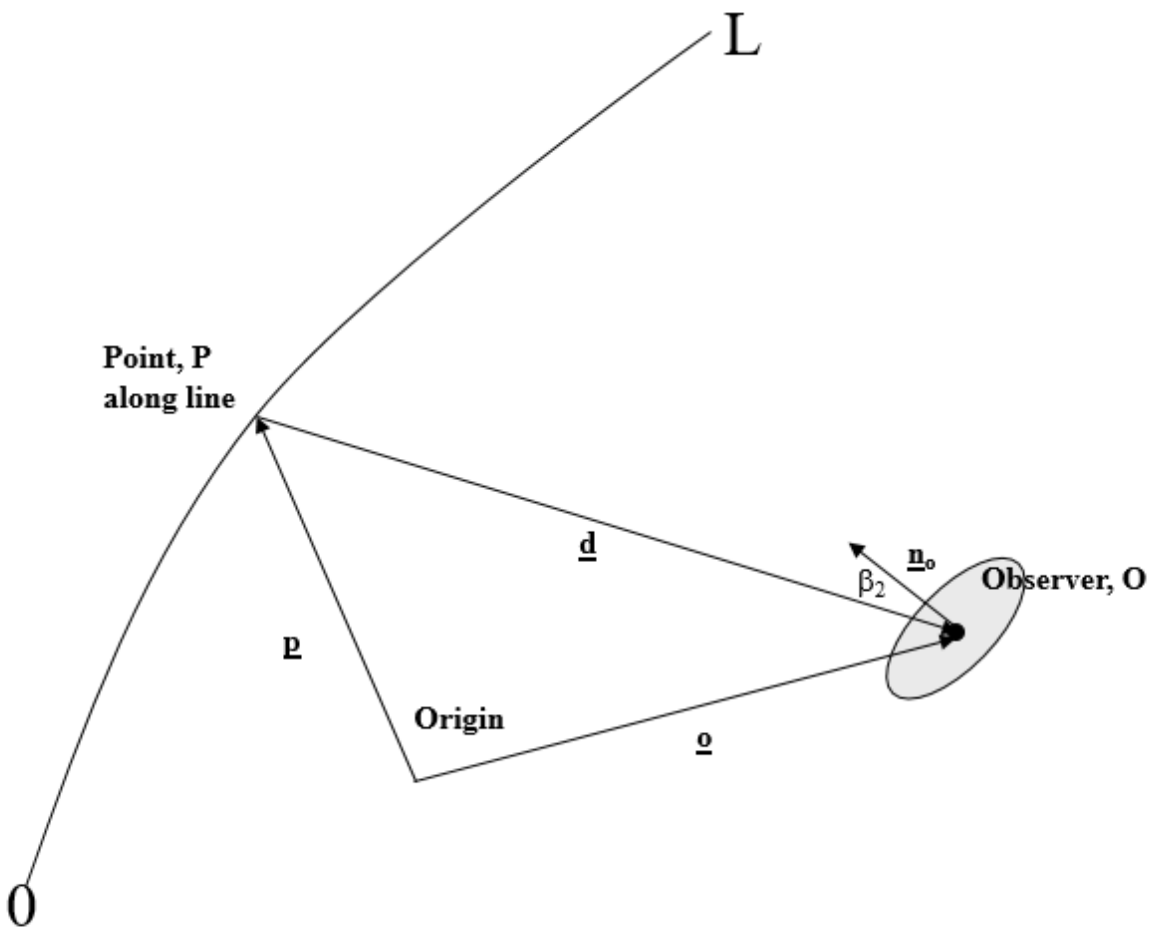

Figure 2. Definition of geometric intensity.

The model for computing geometric intensity is being made up as we go along. It is quite well aligned with the view factor approach.

$$I' = \int_0^L \frac{\tau f(l) cos(\beta_2)}{4\pi d^2} dl \quad (8)$$

d is the vector from the point P to the observer, O (o – p)

β_2 is the angle between the observer plane normal (n_o) and -d

τ is the atmospheric transmissivity, the fraction of radiation not absorbed by the atmosphere

2.2 Input and output

The EXPS view factor models require the following input:

1. Flame geometry. The flame shape is provided as an input to EXPS in the form of a set of circular 'disks'. The exact form is described in Section 4.1.

2. Ambient conditions. The parameters needed to calculate the transmissivity, τ, are supplied. These are the atmospheric humidity, temperature (T) and pressure (P_a).

3. Observer data. EXPS requires the position of the observer. The observer must also be specified to be either a point, or a point on a plane. If on a plane, then EXPS requires the angles of inclination ζ and orientation γ of that plane (these angles are defined in Section 2.3 below). These angles can also be optimised by EXPS to determine the maximum view factor at the point.

They return the following output:

1. View factor (in the range 0 to 1[3])

2. Where applicable, optimised angles γ,ζ for which the view factor has been calculated

[3] The range is 0 to 2 for point observers.

2.3 Observers

An observer has position vector $\underline{o}$ such that:

$$\underline{o} = \begin{bmatrix} o_X \\ o_Y \\ o_Z \end{bmatrix} \quad (9)$$

o_X , o_Y, o_Z are co-ordinates in the global Cartesian co-ordinate system (X,Y,Z).

2.3.1 Planar Observers

The observer normal, $\underline{n}_o$, used extensively in this report is derived from two angles: the observer orientation (γ) and inclination (ζ). The relationship between these is defined as follows:

$$\underline{n}_o = \begin{bmatrix} -\cos\zeta\cos\gamma \\ \cos\zeta\sin\gamma \\ \sin\zeta \end{bmatrix} \quad (10)$$

ζ is thus angle between the observer normal and the horizontal plane. γ is the angle between the projection of the observer normal onto the horizontal plane, and the Y axis. A few examples suffice to describe how ζ and γ affect the normal. When $\zeta = \gamma = 0$, $\underline{n}_o = [-1,0,0]^T$ and the observer lies on the plane $X = o_X$ constant facing upwind. When $\zeta = 0$ and $\gamma = \pi/2$, $\underline{n}_o$ is $[0,1,0]^T$ and the observer lies on the plane $Y = o_Y$ facing towards increasing Y values. When $\gamma = 0$ and $\zeta = \pi/2$, $\underline{n}_o = [0,0,1]^T$ and the observer lies on the plane $Z = o_Z$ facing towards increasing Z values.

2.3.2 Point observers

One simplification of the above model is for the case when an observer is considered to be a point rather than to lie on a plane. In this case, the cos β_2 term in Equation (2) is always unity, and the point is considered to be effectively 'facing' all points on the flame surface:

$$V = \frac{1}{\pi}\iint_S \frac{\tau \max\left(\underline{d}\cdot\underline{n}_p, 0\right)}{d^3} dS \quad (11)$$

This option is allowed for all of the specific flame geometry models described below, but is only explicitly mentioned where it requires a different analysis of the model or allows additional simplification. It was originally introduced to reduce calculation time while still producing conservative results.

2.3.3 Optimization of Planar Observers

We may wish to optimize the facing of planar observers so as to maximize received radiation. In general, for flames represented by plane surfaces (i.e., non-multi point source radiation modelling), this is done by pointing the observer towards the flame along the shortest vector from the observer to the flame surface (by methods described for each individual model, below)[4]. For flames modelled using the multi point source approach (see section 1.1), the optimization is undertaken numerically by pointing the observer along the flame centreline and locating the flame centreline position where the calculated geometric intensity (see equation (8)) at the observer is maximum.

It was also possible prior to PHAST 6.4 to optimize with respect to one only of ζ or γ. This was originally intended for faster optimization when the other angle could confidently be predicted (*e.g.* $\gamma = 0$ when searching downwind). Although it is hard to conceive of a situation where users would wish to optimize one angle and not the other, this functionality has been kept in EXPS, but again using analytical methods for non-multi point source radiation modelling and numerical methods otherwise.

The starting point is the determination of the fully optimized observer normal, $\underline{n}_o^{opt}$ as described for each model below. Our condition for the partially optimized observer will be to minimize (given the constraint of a fixed ζ or γ) the angle

[4] Prior to PHAST 6.4 this optimization involved numeric convergence on a maximum, but significant computational cost. As the difference in radiation is not in general significant (view factor 0.02 or less), the numeric approach has been abandoned.

between it and the fully optimized observer. If the partially optimized (with respect to say ζ) observer has normal $\underline{n}_o^{\zeta,opt}$ then we wish to maximize their dot product as a function of ζ:

$$f(\zeta;\gamma) = \underline{n}_o^{opt} \cdot \underline{n}_o^{\zeta,opt} = \left(n_{Yo}^{opt} \sin\gamma - n_{Xo}^{opt} \cos\gamma\right)\cos\zeta + n_{Zo}^{opt} \sin\zeta \qquad (12)$$

Where γ is the fixed observer orientation. Differentiating and setting this to zero gives the solution:

$$\tan\zeta = \frac{n_{Zo}^{opt}}{n_{Yo}^{opt} \sin\gamma - n_{Xo}^{opt} \cos\gamma} \qquad (13)$$

If the 2nd derivative f ″(ζ;γ) is positive, then the solution in the range -π/2 to π/2 is a minimum and the resultant observer normal will point directly away from the flame. To obtain the maximum, ζ should be shifted by π. However, ζ is constrained[5] to be in the range -π/2 to π/2 and the normal $\underline{n}_{\zeta opt}$ will differ significantly from $\underline{n}_{opt}$.

A similar exercise expressing the dot product as a function of γ leads to a solution for optimized γ to be:

$$\tan\gamma = -\frac{n_{Yo}^{opt}}{n_{Xo}^{opt}} \qquad (14)$$

There are two solutions in the permitted range for γ of -π to π. The maximum is obtained by testing against the 2nd derivative.

2.4 Atmospheric Transmissivity

Atmospheric transmissivity describes the fraction of radiation not absorbed by the atmosphere before it reaches the observer. There are three supported methods[6] for transmissivity calculations. That of Wayne is the only supported method in PHAST / SAFETI. The other methods are available in NEPTUNE.

The method of Wayne (1991) calculates transmissivity from the absorption coefficients for water vapour, $X(H_2O)$, and carbon dioxide, $X(CO_2)$:

$$\tau = 1.006 - 0.01171 \times \log X(H_2O) - 0.02368 \times [\log X(H_2O)]^2 \qquad (15)$$
$$-0.03188 \times \log X(CO_2) + 0.001164 \times [\log X(CO_2)]^2$$

The absorption coefficient for water vapour is given by:

$$X(H_2O) = \frac{2.165 \times P_{wv} \times d}{T} \qquad (16)$$

Where the atmospheric water vapour pressure, P_{wv} , is the product of humidity and saturated vapour pressure at ambient temperature and pressure. The absorption coefficient for carbon dioxide is given by:

$$X(CO_2) = \frac{273 \times d}{T} \qquad (17)$$

The value actually used for transmissivity is allowed minimum and maximum values of 0 and 1[7].

The method of Raj (1977) is:

$$\tau = 1.389 - 0.135 \log(P_{wv} d) \qquad (18)$$

[5] This constraint did not exist in PHAST 6.3 and before, but as EXPS will normally use fully optimized observers (it is no slower than partially or even fixed observers), this is unlikely to be an issue.

[6] A fourth method sets τ = 1 and is used only for verification purposes.

[7] Note that Wayne (1991) suggests distances of between 10 and 1000m, and temperatures between 253 and 313K for this empirical fit. In the absence of a more general fit, the specified minimum and maximum values allow its use outside this range

The final supported method is that of Brzustowski and Somer (1973):

$$\tau = 0.79\left(\frac{1}{r_h}\right)^{\frac{1}{16}}\left(\frac{30.5}{d}\right)^{\frac{1}{16}} \quad (19)$$

where r_h is the (fractional) ambient relative humidity.

3 FLAME DESCRIPTION

This section covers the geometry of the flame shapes, and commonly used methods and properties for the flame and its components.

3.1 Division of Flame Into Disks

The flame shape data provided to EXPS is in the form of a number N ($3 \le N \le 10$) of circular disks (Figure 3).

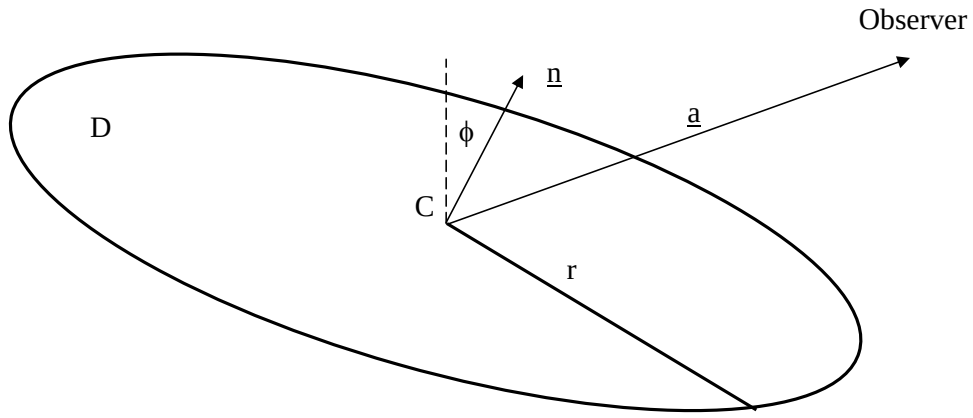

Figure 3. Definition of a disk.

A disk is defined by the following quantities (Figure 3): its centre, C (assumed in plane Y = 0), its radius, r (m), and its tilt or angle between disk and horizontal plane, φ (rad). The tilt is the angle through which the disk is rotated clockwise (looking in positive Y direction) in the vertical plane Y = 0.

3.2 Testing for Points Engulfed By Flame

Given an observer o, then it may be necessary to determine whether it is inside or outside the flame. Given o_Z the along-wind extent of the flame can be determined (see below). If o_X lies in this range, then the crosswind extent of the flame determines whether the observer is engulfed by flame[8, 9].

The crosswind extent of the flame is dependent on specific flame geometry, and is therefore described for each model in Section 4.

3.2.1 Flame Alongwind Extent

To calculate the upwind and downwind extent (X_{min} , X_{max}) of the flame at a specified height, Z, the co-ordinates of the flame boundary in the plane Y = 0 are determined. If successive co-ordinates cross the height Z, then the X co-ordinates are determined by linear interpolation.

The flame (comprising *N* disks) and horizontal plane at height Z intersect if:

[8] At present, the v6.3 algorithm is still used for this determination but is flawed (VI4198, 7897) in the case of non-horizontal API flames. The method described here should be used instead.

[9] To avoid numerical instabilities observed in integral methods employed in view factor calculations (D-11851) for observers very close to the flame surface, an "extended flame engulfment boundary" has been defined where any observer within a limiting distance from the flame surface is assumed to be engulfed (view factor = 1). The limiting distance for the "extended flame engulfment boundary" is currently set to 1% of the characteristic flame size. The characteristic flame size varies with flame type and for example corresponds to flame diameter for fireballs and for cones and cylinders, the minimum of the frustum length and tip diameter.

$$\underset{1\le i\le N}{Min}\left[c_{Zi}+r_i\sin\phi_i\right]<o_Z \qquad (20)$$
$$\underset{1\le i\le N}{Max}\left[c_{Zi}-r_i\sin\phi_i\right]>o_Z$$

Where N is the number of flame disks. For where an intersection occurs, consider a cross-section in the plane Y = 0 of a flame bounded by 2 disks (Figure 4). The horizontal plane can intersect the flame along any of its edges. For any edge (say AC), then we know there is an intersection (at P) if:

$$Min\left[A_Z,C_Z\right]<o_Z \qquad (21)$$
$$Max\left[C_Z,A_Z\right]>o_Z$$

If an edge intersects the ellipse plane, the co-ordinates of the intersection can be found by linear interpolation. By looping through all the flame edges, the maximum upwind (X_{min}) and downwind (X_{max}) intersection points can be determined.

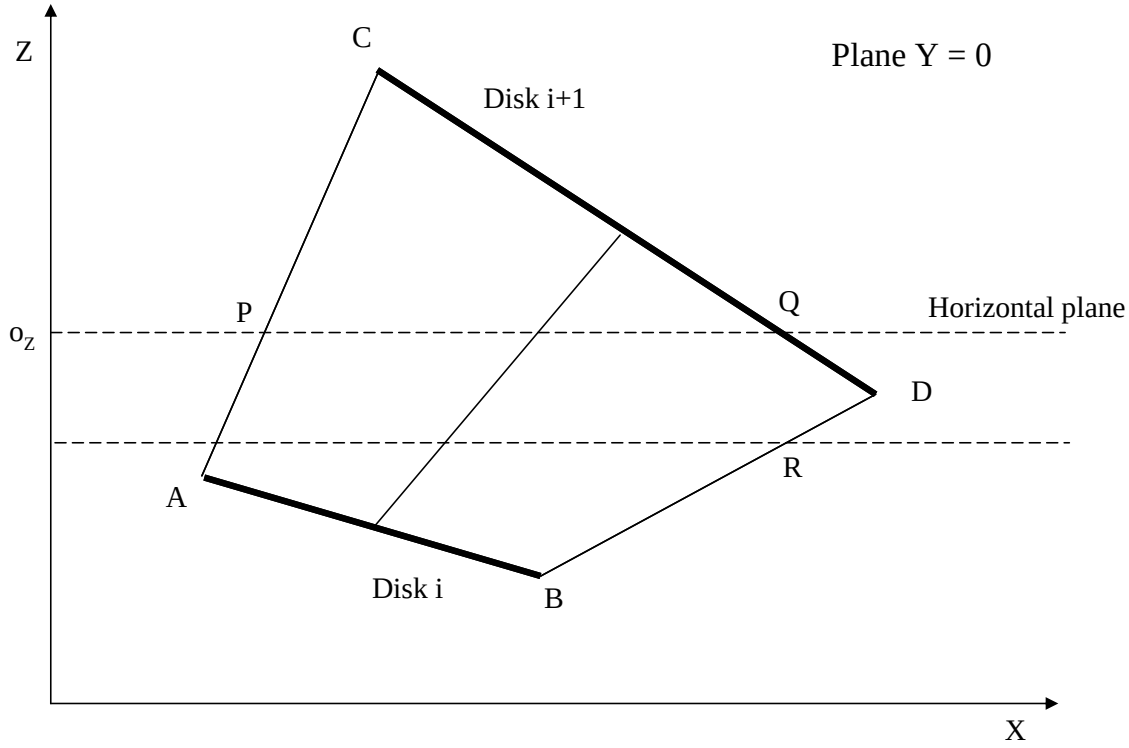

Figure 4. Vertical cross-section (Y=0) through a frustum showing intersection with a horizontal plane

3.2.2 Crosswind Extent

Determination of the flame crosswind extent for given X, Z is dependent on flame geometry. The methods are described in the individual models.

3.3 Relationship Between Observers and Flame Disks

The vector a is from the disk centre to the observer, and the disk unit normal is n:

$$\underline{n}_D=\begin{bmatrix}\sin\phi\\0\\\cos\phi\end{bmatrix} \qquad (22)$$

We define orthogonal unit vectors in the plane of the disk $\underline{e}_x$, $\underline{e}_y$ such that $\underline{e}_x$ lies in the plane Y = 0:

$$\underline{e}_x = \begin{bmatrix} \cos\phi \\ 0 \\ -\sin\phi \end{bmatrix} \quad \underline{e}_y = \begin{bmatrix} 0 \\ 1 \\ 0 \end{bmatrix} \qquad (23)$$

If $\underline{o}_s$ is the position of the projection of the observer $\underline{o}$ onto the disk plane, and $\underline{a}_s$ the vector from the slice centre to $\underline{o}_s$ then:

$$\underline{o}_s = \underline{o} - \underline{b} = \underline{o} - (\underline{a} \cdot \underline{n})\underline{n} \qquad (24)$$

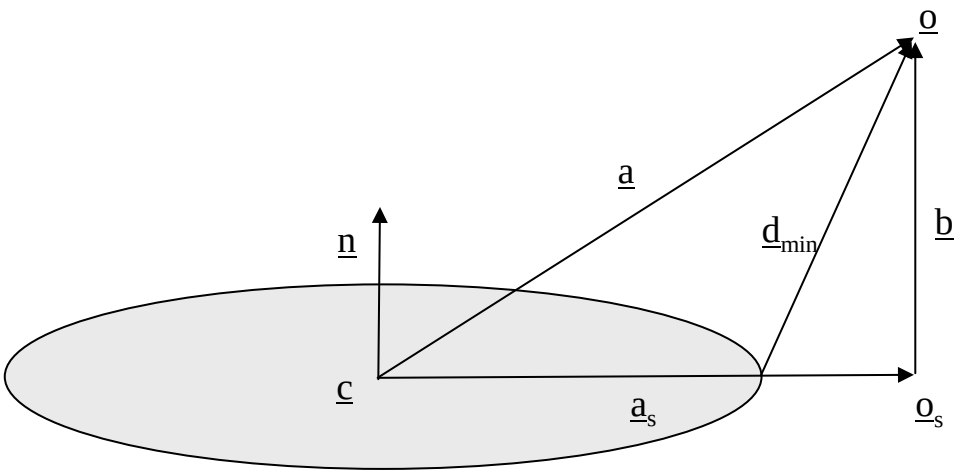

Figure 5. Projection of observer onto plane of slice

The shortest vector, $\underline{d}_{min}$, from disk perimeter to an observer is:

$$\underline{d}_{\min} = \underline{a} - \frac{r}{|\underline{a}_s|}\underline{a}_s \qquad (25)$$

For cases where the projection of the observer onto the disk is coincident with the disk centre all points on the disk circumference are equidistant from the observer, and an arbitrary point on the circumference (x= r, y = 0) is used to determine $\underline{d}_{min}$.

The shortest vector from the disk surface to an observer is $\underline{b}$ if $|\underline{o}_s - \underline{c}| < r$, or $\underline{d}_{min}$ otherwise.

4 VIEW FACTOR CALCULATIONS FOR SPECIFIC FIRE GEOMETRIES

4.1 Flames as Composite Disks

For all the PHAST / SAFETI fire models (POLF, BLEVE, JFAP, JFSH), the flame is described by the surface created by joining the perimeters of a number of disks (*e.g.* Figure 6). The specific geometry assumed for each model can be found in that model's documentation, but to summarise:

- **POLF (Pool fire)**. Three disks, where φ = 0 for all disks. The radius of disks one and 2 are equal, while that for disk 3 is zero. Disks 2 and 3 are concentric, and the surface defined by these therefore define a circle. The pool is modelled as a tilted cylinder (Section 4.4) topped by a circle (Section 4.3). Note the base of the flame is not considered part of the surface (*i.e.* the view factor below pool fires is zero).
- **BLEVE**. Ten disks, where φ = 0 for all disks. The radii of the first and last disks are zero. This representation of the BLEVE surface is ignored for the radiation calculations[10], which use the Sphere model (Section 4.5)

[10] Prior to PHAST 6.4 this description was used, as all flames were modelled as jointed frusta.

- **JFSH (Shell jet fire).** Four disks, where φ are equal for all. The centres for disks 1 and 2 are coincident, as are those for disks 3 and 4. The line joining the disk centres is perpendicular to the disk planes. The radii of the first and last disks are zero. Modelled as circles (Section 4.3) top and bottom separated by a cone (Section 4.6).
- **JFAP (API jet fire).** Ten disks, modelled as nine frusta defined by successive pairs of disks. For horizontal fires, φ is equal for all disks and the flame is modelled as nine frusta (Section 4.2) or (in the case of horizontal fires) cones (Section 4.6).

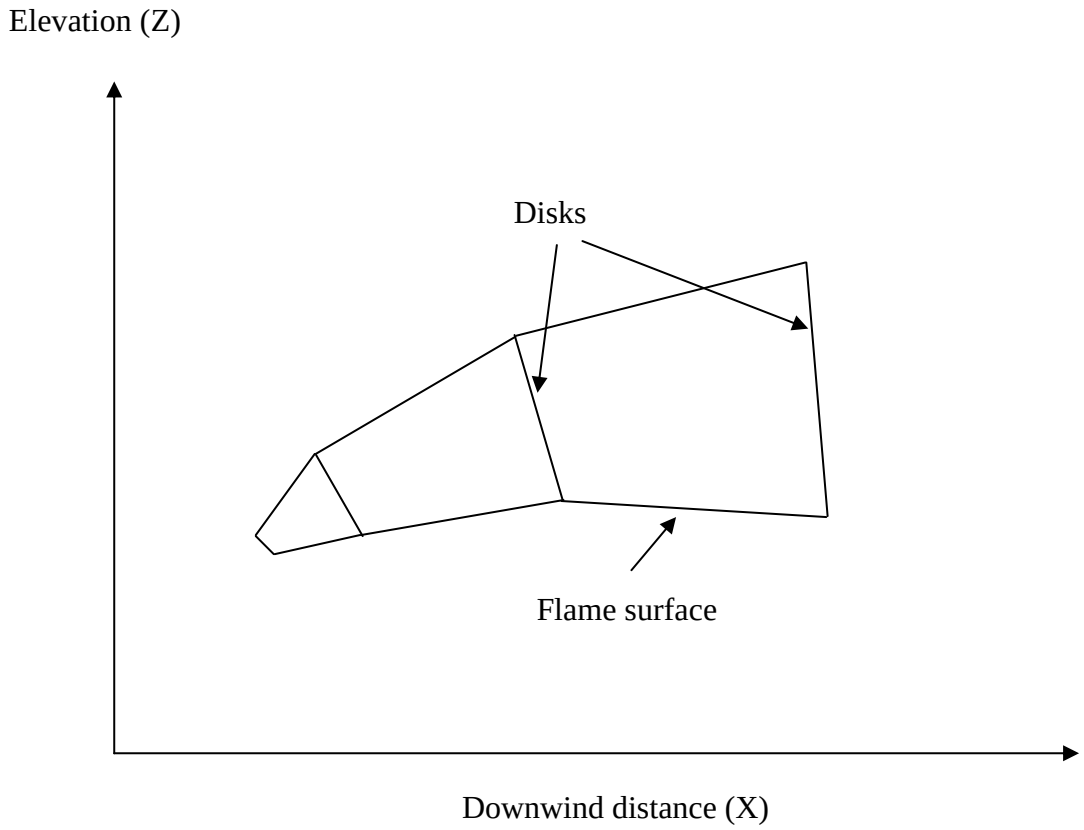

Figure 6. Flame surface comprising jointed disks (shown in vertical plane Y = 0)

4.2 Frustum Model

This model allows calculation of the view factor for flames whose surfaces are described by a frustum, that is the surface defined by connecting the perimeters of two disks. This model is used for non-horizontal API jet fires; all other fires have simpler geometries and use simpler models.

In developing the theory, the intention is to firstly define the flame surface using two parameters h and θ. Secondly, to derive expressions for the vectors $\underline{p}$, and $\underline{n}_p$ as described in Section 2. Thirdly, to derive expressions for calculating the integral limits as a function of the inner independent variable, θ.

4.2.1 Flame Geometry and Parametric Description

For this model, the flame surface is that defined by connecting the perimeters of two circular disks, D_0 and D_1 (Figure 7). The disks themselves are not part of the surface.

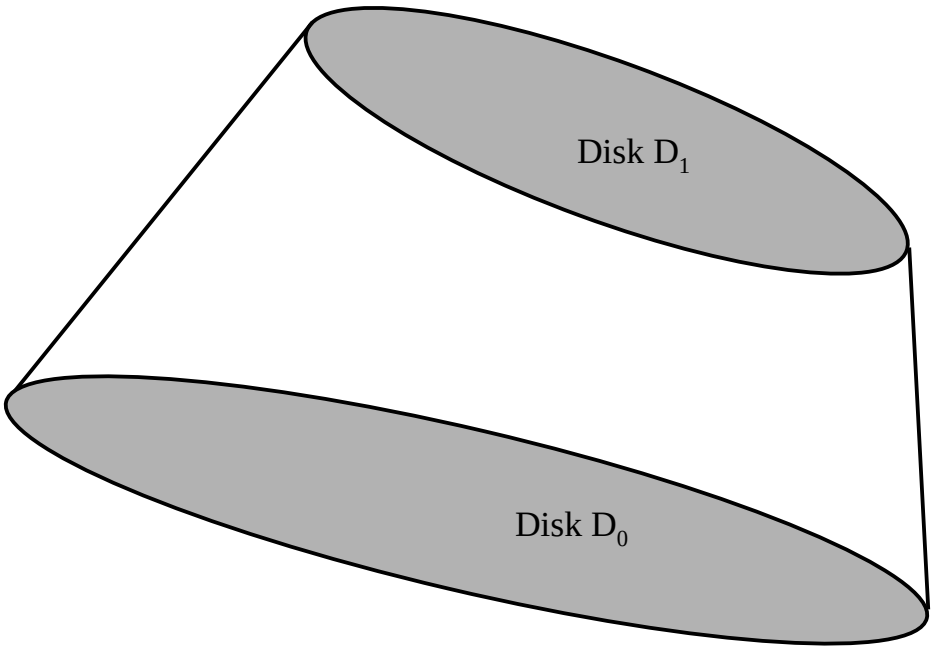

Figure 7. Flame surface as a frustum defined by two disks.

The frustum surface is given a parametric description in terms of a dimensionless height, h ($0 \le h \le 1$) and angle θ ($-\pi \le \theta < \pi$). The height, h defines another circular disk 'slice', D_h , through the frustum. The orientation φ_h , and centre position vector $\underline{c}_h$ of this slice are obtained by linear interpolation between the top and bottom frustum defining disks:

$$\underline{c}_h = \underline{c}_0 + h\left(\underline{c}_1 - \underline{c}_0\right) \quad (26)$$

$$\phi_h = \phi_0 + h\left(\phi_1 - \phi_0\right) \quad (27)$$

For the radius, r_h , the product of r cosφ must be linear[11]:

$$r_h = \frac{r_1 \cos\phi_1 + h\left(r_2 \cos\phi_2 - r_1 \cos\phi_1\right)}{\cos\phi_h} \quad (28)$$

r_1 is the radius of the lower disk
r_2 is the radius of the upper disk
r_h is the radius of the slice

Once we have defined the slice, it becomes convenient to use the disk D_h plane as a reference with its local co-ordinate system (x,y). The next stage is to determine the angle μ subtended by the projected observer and the y = 0 (Figure 8).

[11] Consideration of cases where $r_1 = r_2$, $\varphi_1 \neq \varphi_2$ illustrates why this is the case. A similar expression can be derived using sines, for use when the fire is oriented horizontally

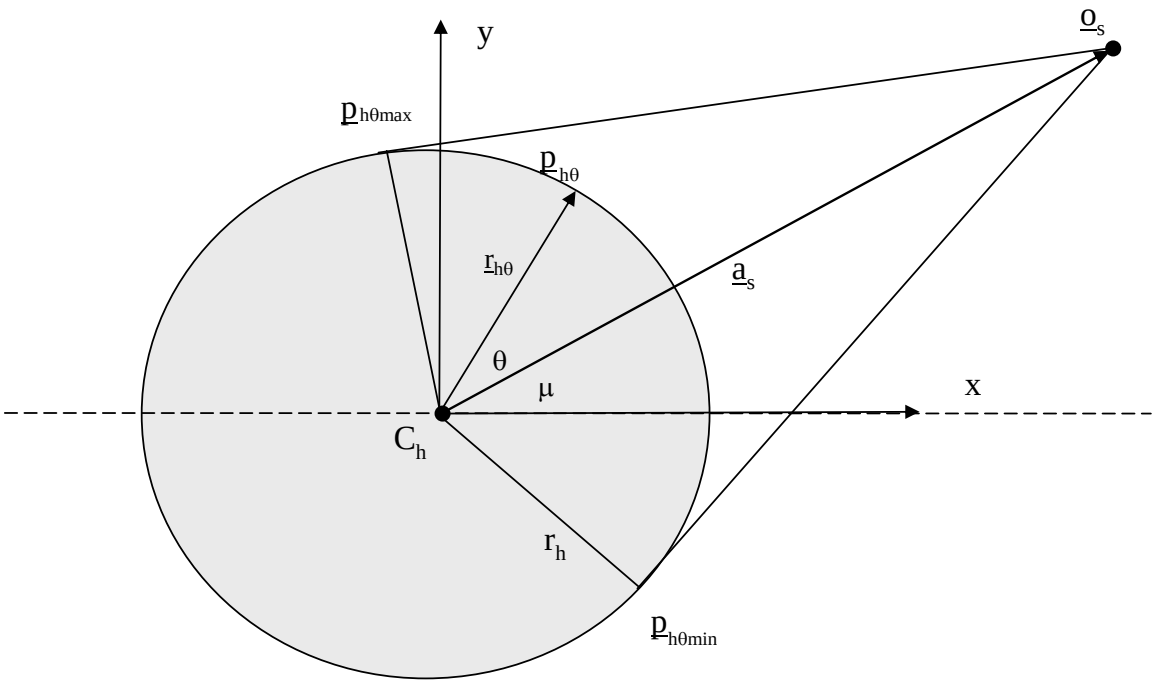

Figure 8. Parameterisation using θ in plane of slice.

Then μ must satisfy:

$$\cos\mu = \frac{\underline{a}_s \cdot \underline{e}_x}{a_s} \qquad (29)$$

The second parameter, θ ($-\pi \le \theta < \pi$), defines the point $\underline{p}_{h\theta}$ along the circumference of the slice, with θ = 0 a point on $\underline{a}_s$. In terms of local Cartesian co-ordinates (x,y) relative to the grid centre, the radial vector from the slice centre to any point P on its surface is given by:

$$\underline{r}_{h\theta} = \begin{bmatrix} r_x \\ r_y \end{bmatrix} = r_h \begin{bmatrix} \cos(\theta+\mu) \\ \sin(\theta+\mu) \end{bmatrix} \qquad (30)$$

These local co-ordinates are transformed into the global (X,Y,Z) system using the local axes unit vectors:

$$\underline{r}_{h\theta} = r_x \underline{e}_x + r_y \underline{e}_y \qquad (31)$$

The position vector $\underline{p}$ is then simply:

$$\underline{p}_{h\theta} = \underline{c}_h + \underline{r}_{h\theta} \qquad (32)$$

Another required quantity for the model is the vector normal to the flame surface at P, $\underline{n}_p$. Let $\underline{e}_\theta$ be the 'flame edge' vector from the point $\underline{p}_{0\theta}$ to $\underline{p}_{1\theta}$ (*i.e.* between corresponding points on the frustum upper and lower disks). For a given θ, this vector passes through all points $\underline{p}_{h\theta}$ on the frustum surface. Now the normal $\underline{n}_p$ must by definition be perpendicular to $\underline{e}_\theta$, and in the same plane as $\underline{e}_\theta$ and $\underline{r}_{h\theta}$ (Figure 8).

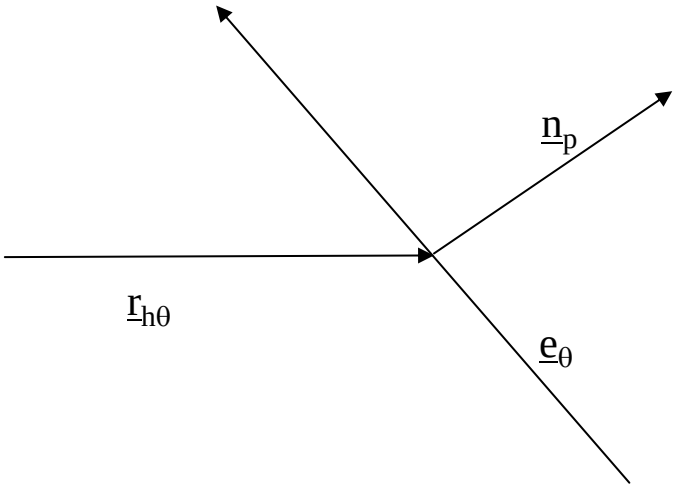

Figure 9. Determination of normal to flame surface.

The vector normal to the plane defined by the three vectors is the cross product ($r_{h\theta} \times \underline{e}_\theta$) of the two known vectors, $\underline{r}_{h\theta}$, and $\underline{e}_\theta$. The vectors $\underline{e}_\theta$, $r_{h\theta} \times \underline{e}_\theta$ and $\underline{n}_p$ are all perpendicular, so we can find $\underline{n}_p$ as the cross product of the other two:

$$\underline{n}_p = \underline{n}_{h\theta} = \frac{\underline{e}_\theta \times (\underline{r}_{h\theta} \times \underline{e}_\theta)}{\left|\underline{e}_\theta \times (\underline{r}_{h\theta} \times \underline{e}_\theta)\right|} \qquad (33)$$

4.2.2 Integration Over Flame Surface

We now have a parametric equation for any point on the flame surface, and for the normal to the surface at that point. The next step is to integrate this over the flame surface to compute the view factor. An area dS of the flame surface can be expressed as dH × dA, where dA is the arc length and dH the slant height. We can write:

$$dA = r_h d\theta \qquad (34)$$
$$dH = e_\theta dh$$

Consequently the integral can be written:

$$V = \frac{1}{\pi} \int_{h=0}^{1} \int_{\theta_{\min}}^{\theta_{\max}} \frac{\tau \max(\underline{d}_{h\theta} \cdot \underline{n}_{h\theta}, 0) \max(-\underline{d}_{h\theta} \cdot \underline{n}_o, 0)}{d^4} r_h e_\theta d\theta dh \qquad (35)$$

4.2.3 Integral Limits

For h, the outer limits are set always to 0 and 1. For the integration with respect to θ, the limits θ_{min} and θ_{max} must be established as functions of h. For an observer that lies in the plane of a slice, these limits are illustrated in Figure 8 and it is clear that:

$$\cos\theta_{\min} = \cos\theta_{\max} = \frac{r_h}{a_s} \qquad (36)$$
$$\theta_{\max} = -\theta_{\min}$$

As the observer moves away from the plane of the slice, for a non-cylindrical (*i.e.* $r_1 \neq r_2$) frustum the proportion of the slice perimeter visible changes, and the first condition no longer holds[12]. The condition to be satisfied at θ_{max} and θ_{min} is that of Equation (6) which is analytically hard, but can be solved numerically using standard methods. The limits for the search are $\theta_{max} \leq \theta \leq \pi$.

[12] In the extreme case of a 'flattened' frustum (*e.g.* top of a pool fire), once off the plane of the slice the entire perimeter is visible to the observer.

4.2.4 Shortest Vector To Observer

This method is used to point the observer towards the flame in order to estimate the optimum angles ζ and γ at which radiation received is maximised.

Using as a starting point the shortest vector from a disk perimeter to an observer, $\underline{d}_{min}$ (25) we can express its magnitude as:

$$d_{\min}{}^2 = b^2 + (a_s - r)^2 \qquad (37)$$

For a frustum, d_{min}^2 will vary as a function of h, the parametric descriptor of a particular slice. In order to find the minimum d_{min}, we differentiate the above expression with respect to h:

$$\frac{d}{dh}\left(d_{\min}^2\right) = 2bb' + 2(a_s - r)\left(\frac{aa' - bb'}{a_s} - r'\right) \qquad (38)$$

The derivatives a' , b' , and r' are simply determined from the parametric description of the frustum derived earlier (Equations (24), (27), and (28)). For radius this is:

$$r' = \frac{1}{\cos\phi_h}\left\{r_2\cos\phi_2 - r_1\cos\phi_1 + (\tan\phi_h)(\phi_2 - \phi_1)\left[r_1\cos\phi_1 + h(r_2\cos\phi_2 - r_1\cos\phi_1)\right]\right. \qquad (39)$$

If $\Delta\underline{c}$ is the vector from $\underline{c}_1$ to $\underline{c}_h$ then by the cosine rule, the expression for a satisfies:

$$a^2 = \Delta c^2 + a_1^2 - 2\Delta\underline{c}\cdot\underline{a}_1 \qquad (40)$$

$$a^2 = h^2\left|\underline{c}_2 - \underline{c}_1\right|^2 + a_1^2 - 2h(\underline{c}_2 - \underline{c}_1)\cdot\underline{a}_1$$

And therefore the product aa' is

$$aa' = h\left|\underline{c}_2 - \underline{c}_1\right| - (\underline{c}_2 - \underline{c}_1)\cdot\underline{a}_1 \qquad (41)$$

The value, h_{min} , for which d_{min}^2 is a minimum is found by determining the root of this equation between 0 and 1 (the top and bottom of the frustum) using standard numerical methods. Given h_{min}, the shortest vector $\underline{d}$ to the observer can be determined from the perimeter of the slice defined by h_{min} (25). For a frustum with no root in the region 0 to 1, h_{min} is set to 0 or 1, according to which has smaller $|\underline{d}|$[13].

4.2.5 Crosswind Extent

The crosswind extent of the flame is used for the determination of whether an observer is inside or outside the flame, and for ellipse calculations. Consider a point Q on the flame boundary, then we wish to find Q_Y given Q_X and Q_Z. But Q can also be described as being on a slice through the frustum defined by parametric h, where:

$$\underline{n}_h\cdot(\underline{q} - \underline{c}_h) = 0 \qquad (42)$$

$\underline{n}_h$ is the normal to the slice
$\underline{q}$ is the position vector of Q

This allows us to determine that h satisfies:

[13] Note that when determining d/dh (dmin2), it is important that this is calculated for the same edge for all h. Under certain circumstances (VI7488) the projected observer can 'cross' the slice centre, in which case the distance to the 'far' edge is required and the d_{min}^2 equation should have a (a_s + r) term, and its derivative be modified accordingly.

$$\tan\phi_h = -\frac{A - \phi_h\left(c_{Z1} - c_{Z0}\right)}{B - \phi_h\left(c_{X0} - c_{X0}\right)} \quad (43)$$

where

$$A = \left(a_Z - c_{Z1}\right)\left(\phi_1 - \phi_0\right) + \phi_0\left(c_{Z1} - c_{Z0}\right)$$

$$B = \left(a_X - c_{X1}\right)\left(\phi_1 - \phi_0\right) + \phi_0\left(c_{X1} - c_{X0}\right)$$

This is solved for φ_h numerically using standard methods. If $0 \le h \le 1$, then the given point intersects the flame and the crosswind extent, Q_Y , can be determined from the slice through the frustum:

$$Q_Y^2 = r_h^2 - \left|\underline{a} - \underline{c}_h\right|^2 \quad (44)$$

4.3 Circle Model

The Circle model calculates view factor for a surface defined by a single disk. This model is used for the top of pool fires, and for the top and bottom of Shell jet fires.

4.3.1 Flame Geometry and Parametric Description

The flame geometry is that of a single disk, as illustrated in Figure 10. The local origin is at the centre of the disk, the local x axis is the line joining the origin to the observer projection onto the disk plane[14], the local y axis is orthogonal to the x axis and the flame disk normal, $\underline{n}_f$. The flame normal is therefore the local z axis. We can calculate the observer projection onto the flame surface (*i.e.* disk) plane, $\underline{o}_f$, from Equation (25), and then:

$$\underline{e}_x = \frac{\underline{o}_s - \underline{c}}{\left|\underline{o}_s - \underline{c}\right|} \qquad (45)$$

$$y = \underline{n}_D \times \underline{e}_x$$

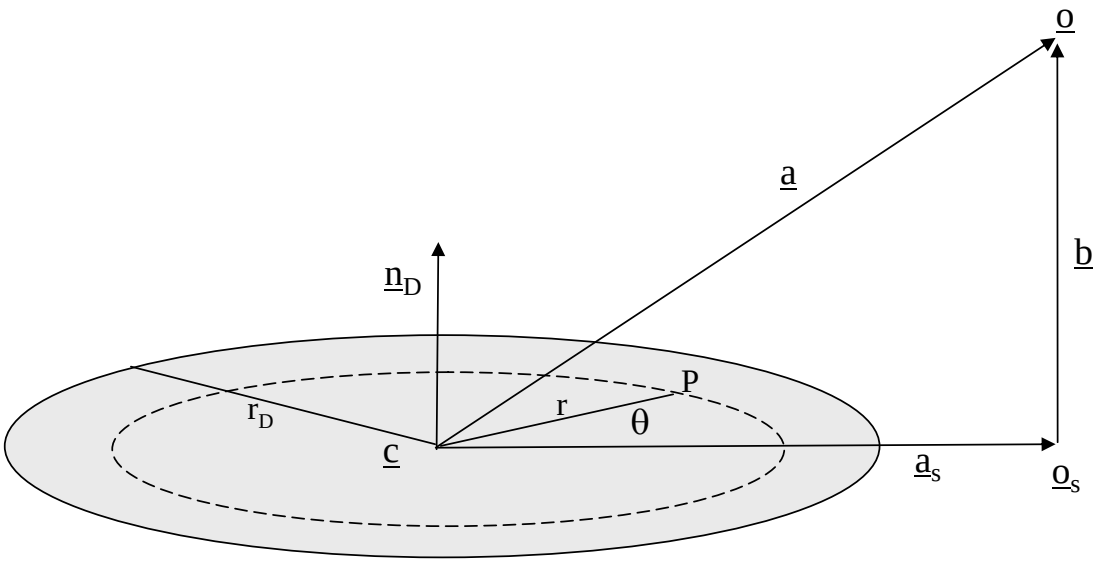

Figure 10. Geometry of Circular Disk Model

A point P on the flame surface is parameterised in terms of radius r ($0 \le r \le r_D$) and angle θ ($-\pi \le \theta \le \pi$), where θ is the rotation in the positive y direction and r_D the circle radius. The position vector of $\underline{p}_{r\theta}$ is:

$$\underline{p}_{r\theta} = \underline{c} + r_D\left(\cos\theta \underline{e}_x + \sin\theta \underline{e}_y\right) \qquad (46)$$

4.3.2 Integration Over Flame Surface

An incremental area dS of the flame surface can be expressed as:

$$dS = rd\theta dr \qquad (47)$$

Consequently the integral can be written:

$$V = \frac{1}{\pi}\int_{r=0}^{r_D}\int_{\theta_{\min}}^{\theta_{\max}} \frac{\tau\left(\underline{d}_{r\theta}\cdot\underline{n}_D\right)\max\left(-\underline{d}_{r\theta}\cdot\underline{n}_o, 0\right)}{d^4} rd\theta dr \qquad (48)$$

The first dot product does not have to be tested at all points to see if it greater than zero, as if it is positive for one point (say the disk centre) then it is always positive.

[14] If this projection is coincident with the centre, then the x axis is arbitrarily set to be the intersection of the global plane Y= 0 with the disk.

4.3.3 Integral Limits

The outer integral limits are always taken to be 0 and r_D , the flame radius. The inner integral limits must be calculated as a function of θ. In general, an observer 'above' the plane is visible from the entire flame surface is visible to an observer, consequently no limits need be established for the surface being obscured due to curvature.

4.3.4 Shortest Vector To Observer

The shortest vector to an observer is as described for a single disk (Section 3.3).

4.4 Tilted Cylinder Model

The Tilted Cylinder model calculates the view factor for a surface defined by two disks of equal radius and inclination φ = 0. This model is used for the lower part of pool fires only.

4.4.1 Flame Geometry and Parametric Description

The model is constructed from an open cylinder with horizontal end disks (Figure 11). The axis of the cylinder is tilted away (in the positive X direction) from the vertical through an angle α_{max}[15]

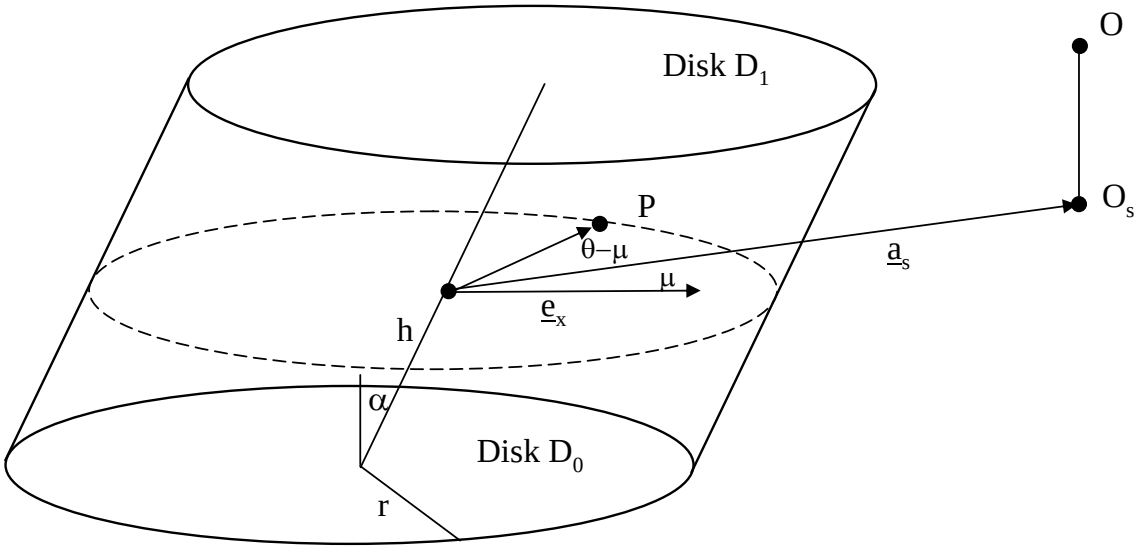

Figure 11. Tilted cylinder model

The centres of the two disks are known, so α_{max} can be calculated as:

$$\tan \alpha_{\max} = \frac{c_{X1} - c_{X0}}{c_{Z1} - c_{Z0}} \quad (49)$$

As per the frustum model, parameterisation is in terms of a dimensionless height, h, and an angle θ. The height h ($0 \le h \le 1$) defines the horizontal slice through the flame, which has the centre $\underline{c}_h$:

$$\underline{c}_h = \underline{c}_0 + h(\underline{c}_1 - \underline{c}_0) \quad (50)$$

The angle μ describing the angle between the x axis and the vector $\underline{a}_s$ from the slice centre to the observer projected onto the slice plane satisfies:

$$\cos \mu = \frac{\underline{a}_s \cdot \underline{e}_x}{a_s} \quad (51)$$

The other parameter, θ ($-\pi \le \theta \le \pi$) describes the rotation in the direction of increasing y around the slice from the x axis. The position of a general point on the surface is therefore:

[15] Note α_{max} should not to be confused with the disk inclination, φ, which is zero for both disks.

$$\underline{p}_{h\theta} = \underline{c}_h + \underline{r}_{h\theta} = \underline{c}_h + r\begin{bmatrix}\cos\theta\\ \sin\theta\\ 0\end{bmatrix} \quad (52)$$

For the normal $\underline{n}_p$ to the flame surface, consider first the downwind extreme of the flame slice. The normal is the radial vector $\underline{r}_{h\theta}$ rotated through the angle α_{max}. For the crosswind extent of the flame, the normal is just the radial vector. Generalising this, we must rotate $r_{h\theta}$ through an angle α:

$$\alpha = \alpha_{max}\cos\theta \quad (53)$$

Therefore we can say:

$$\underline{n}_{h\theta} = \begin{bmatrix}\cos\theta\cos\alpha\\ \sin\theta\cos\alpha\\ -\sin\alpha\end{bmatrix} \quad (54)$$

4.4.2 Integration Over Flame Surface

An area dS of the flame surface can be expressed as dH × dA, where dA is the arc length and dH the slant height. We can write:

$$dA = rd\theta \quad (55)$$
$$dH = \left|\underline{c}_2 - \underline{c}_1\right| dh$$

Consequently the integral can be written:

$$V = \frac{r\left|\underline{c}_1 - \underline{c}_0\right|}{\pi}\int_{h=0}^{1}\int_{\theta_{min}}^{\theta_{max}} \frac{\tau\max\left(\underline{d}_{h\theta}\cdot\underline{n}_{h\theta},0\right)\max\left(-\underline{d}_{h\theta}\cdot\underline{n}_o,0\right)}{d^4} d\theta dh \quad (56)$$

4.4.3 Integral Limits

As described in Section 4.2.3 for the Frustum model, the inner integral limits θ_{max} and θ_{min} are given by:

$$\cos\left(\mu - \theta_{min}\right) = \cos\left(\theta_{max} - \mu\right) = \frac{r}{a_s} \quad (57)$$
$$\theta_{max} + \theta_{min} = 2\mu$$

4.4.4 Shortest Distance

For a flame with no tilt (α = 0), the shortest vector, $\underline{d}_{min}$, from the flame surface to a point (typically the observer) is determined as the shortest vector from a horizontal slice through the flame:

$$\underline{d}_{min} = \underline{o} - \underline{c}_h - \frac{r}{\left|\underline{a}_s\right|}\underline{a}_s \quad (58)$$

The slice (*i.e.* value of h) to use is determined solely from the vertical co-ordinate of the observer:

$$h = 0 \qquad o_{|Z} \le c_{Z0}$$
$$h = 1 \qquad o_Z \ge c_{Z1}$$
$$h = \frac{o_Z - c_{Z0}}{c_{Z1} - c_{Z0}} \qquad otherwise$$

(59)

For $\alpha \neq 0$, the generalised method described for the frustum model is used (Section 4.2.4)[16].

4.5 Sphere Model

In versions of EXPS prior to PHAST 6.4, BLEVEs were described by means of a series of 10 disks with φ = 0 approximating to a sphere. While this has been retained as the form of the input data, the Sphere model uses only the top and bottom disks to calculate the BLEVE radius and centre elevation.

Note that while this approach is used for all BLEVE calculations, for optimized and point observers it is possible to simplify the model even further so it can be expressed as a single integral. This method is documented in 0 and may be implemented in future releases.

4.5.1 Flame Geometry And Parametric Surface Description

One advantage in developing a specific sphere model is its symmetry. We can choose our reference axes (x,y,z) such that the observer plane is horizontal and (if it intersects the BLEVE at all) slices through the BLEVE. The observer y co-ordinate is zero. The BLEVE geometry itself is represented simply by the radius r (Figure 12), the centre is assumed to be at the origin.

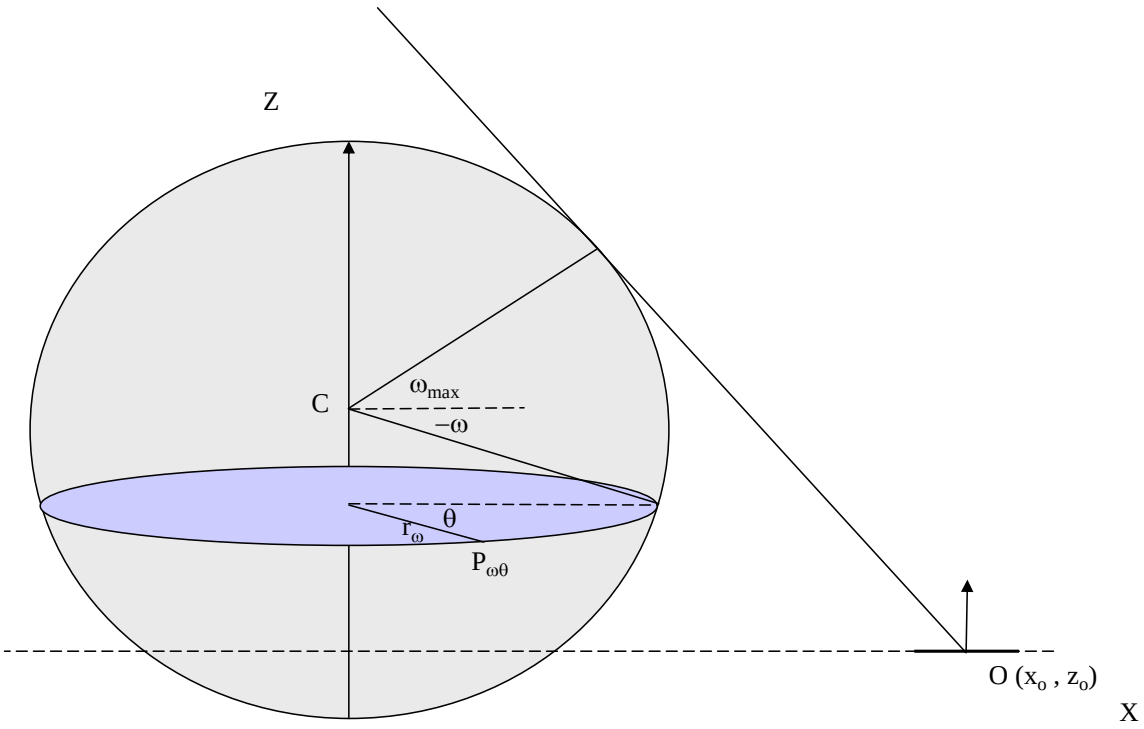

Figure 12. Sphere model

The perpendicular distance from sphere centre to observer plane must be determined from:

$$o_z = -\left(-\underline{a}\right) \cdot \underline{n}_o$$

(60)

o_z is the observer z co-ordinate
$\underline{a}$ is the vector from the sphere centre to the observer
$\underline{n}_o$ is the observer normal (= unit vector in the z direction)

[16] An analytical solution should not be too difficult to derive for this case, but this hasn't been done due to shortage of time.

The orthogonal local axes $\underline{e}_x$, $\underline{e}_y$ and $\underline{e}_z$ are simply:

$$\underline{e}_z = \underline{n}_o$$
$$\underline{e}_y = \frac{\underline{e}_z \times \underline{a}}{|\underline{e}_z \times \underline{a}|} \qquad (61)$$
$$\underline{e}_x = \underline{e}_y \times \underline{e}_z$$

The parametric description of the sphere surface is simple. Given an elevation angle, ω, ($-\pi/2 \le w \le \pi/2$) and rotation angle θ ($-\pi \le \theta \le \pi$), the position vector $\underline{p}_{\omega\theta}$ at any point P on the surface, and the normal to the surface $\underline{n}_{\omega\theta}$ are given by:

$$\underline{p}_{\omega\theta} = r\underline{n}_{\omega\theta} = r\begin{bmatrix}\cos\omega\cos\theta\\ \cos\omega\sin\theta\\ \sin\omega\end{bmatrix} \qquad (62)$$

4.5.2 Integration Over Flame Surface

We can express a small increment in the flame surface area in terms of the two parameters:

$$dS = rr_\omega d\theta d\omega \qquad (63)$$

Now if $\underline{d}_{\omega\theta}$ is the vector from $\underline{p}_{\omega\theta}$ to the observer, then the integral can be expressed as:

$$V = \frac{r}{\pi}\int_{\omega_{\min}}^{\omega_{\max}}\int_{\theta_{\min}}^{\theta_{\max}} \frac{\tau}{d^4}\left(\underline{d}_{\omega\theta}\cdot\underline{n}_{\omega\theta}\right)\left(-\underline{d}_{\omega\theta}\cdot\underline{e}_z\right)r_\omega d\theta d\omega \qquad (64)$$

Note that the observer normal, $\underline{n}_o$ has been replaced in this expression with the unit z vector, $\underline{k}$, as the observer plane by definition faces upwards according to our local axes.

4.5.3 Integral Limits

For the outer integral limits, ω_{min} satisfies:

$$r\sin\omega_{\min} = o_z \qquad (65)$$

where o_z is the observer Z co-ordinate. If the observer plane does not intersect the sphere (*i.e.* $|o_z| > r$), then either the flame is hidden behind the observer plane (V = 0), or the entire BLEVE is visible. In this latter case ω_{min} is $-\pi/2$.

The ω_{max} is obtained by drawing a tangent to the BLEVE in the plane y = 0 through O. From Figure 13, we have:

$$a\sin\psi = -o_z$$
$$\cos(\omega_{\max} + \psi) = \frac{r}{a} \qquad (66)$$

We solve to get:

$$\omega_{\max} = \sin^{-1}\left[\frac{o_z}{a}\right] + \cos^{-1}\left[\frac{r}{a}\right] \qquad (67)$$

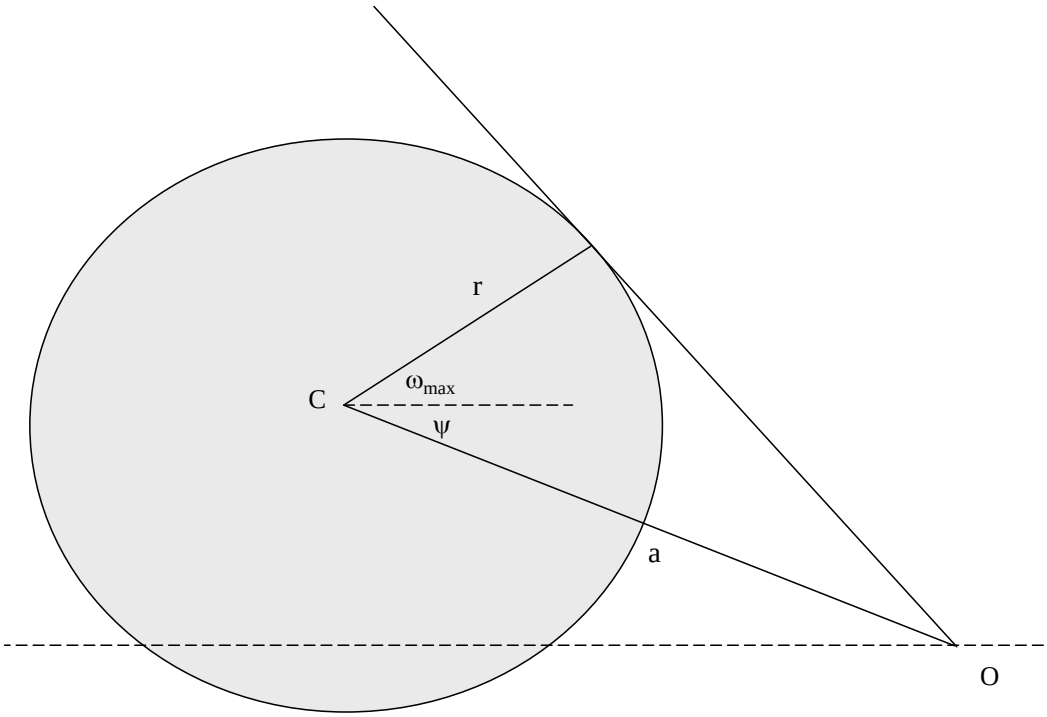

Figure 13. Integral limits for BLEVEs

As for the other models, the condition for the inner limits that of Equation (6). Substituting in the previously derived terms yields the solution:

$$\cos\theta_{\max} = \frac{r - o_z \sin\omega}{o_x \cos\omega} \qquad (68)$$

$$\theta_{\min} = -\theta_{\max}$$

4.5.4 Shortest Vector To Observer

Clearly, this is the vector of length |a – r| from the observer towards the sphere centre. This is also the vector along which an observer facing will receive maximum radiation.

4.6 View Factor for a Cone

The Cone model describes the case where adjacent disks have the same inclination and line joining the disk centres is normal to the plane of the disks. The model is used for the central section of the Shell jet fire model, and for special cases of the API jet fire (specifically horizontal releases).

4.6.1 Flame Geometry

The Cone model is illustrated in
Figure 14. A local co-ordinate system (x,y,z) is chosen such that the centre of Disk 0 is at the origin, the vector from the centre of the bottom to the top disk is the z axis, and the x axis is from the centre of the bottom disk to the observer projected onto the plane of that disk.

In local terms, the observer is defined by co-ordinates o_x, o_z , where:

$$o_z = \underline{a}_0 \cdot \underline{n}_0 \qquad (69)$$

$\underline{a}_0$ is the vector from the centre of Disk 0 to the observer
$\underline{n}_0$ is the normal to Disk 0

Then o_x is easily determined as:

$$o_x^2 = a_1^{\,2} - o_z^2 \qquad (70)$$

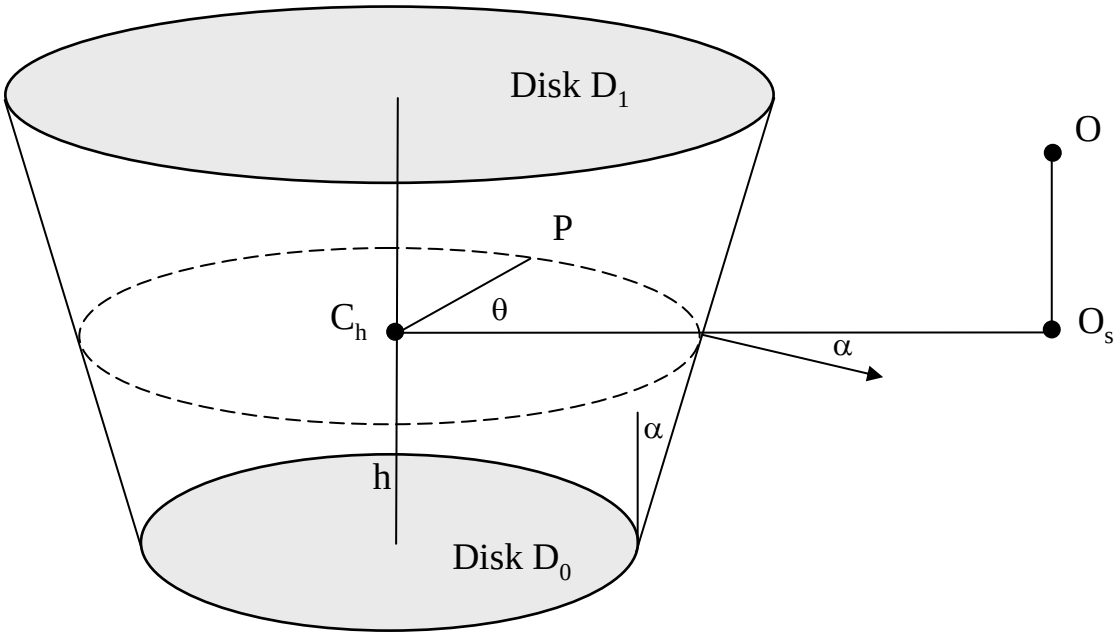

Figure 14. Cone view factor model

The local axes $\underline{e}_x$ and $\underline{e}_z$ are simply

$$\underline{e}_x = \frac{\underline{a}_s}{a_s} \qquad \underline{e}_z = \underline{n}_D \tag{71}$$

and the z axis is orthogonal to these. The observer normal, $\underline{n}_o$ is expressed into local co-ordinates by solving the following linear system by standard methods:

$$\left[\underline{e}_x \quad \underline{e}_y \quad \underline{e}_z\right]\underline{n}_{o,local} = \underline{n}_o \tag{72}$$

4.6.2 Parametric Description

The position of a general point, P, on the surface is defined by dimensionless parameters h ($0 \le h \le 1$) and θ ($-\pi \le \theta \le \pi$). The radius r_h of the horizontal slice defined by h is:

$$r_h = r_0 + h(r_1 - r_0) \tag{73}$$

The position vector for P is:

$$\underline{p}_{h\theta} = h\underline{c}_1 + r_h\left(\cos\theta\,\underline{e}_x + \sin\theta\,\underline{e}_y\right) = \begin{bmatrix} r_h\cos\theta \\ r_h\sin\theta \\ hH \end{bmatrix} \tag{74}$$

H is distance from the centre of Disk 0 to Disk 1

The normal to the surface at P is the radial vector from centre to flame edge rotated through an angle α. Note that α is independent of h or θ:

$$\tan\alpha = \frac{r_2 - r_1}{H} \quad (75)$$

The normal $\underline{n}_\theta$ is given by:

$$\underline{n}_\theta = \begin{bmatrix} \cos\theta\cos\alpha \\ \sin\theta\cos\alpha \\ -\sin\alpha \end{bmatrix} \quad (76)$$

4.6.3 Integration Over Flame Surface

An area dS of the flame surface can be expressed as dE × dA, where dA is the arc length and dE the slant height. We can write:

$$dA = r_h d\theta \quad (77)$$
$$dE = dh\frac{H}{\cos\alpha}$$

Consequently the integral can be written:

$$V = \frac{H}{\pi\cos\alpha}\int_{h=0}^{1}\int_{\theta_{\min}}^{\theta_{\max}} \frac{\tau\max\left(\underline{d}_{h\theta}\cdot\underline{n}_{h\theta},0\right)\max\left(-\underline{d}_{h\theta}\cdot\underline{n}_o,0\right)}{d^4} r_h d\theta dh \quad (78)$$

4.6.4 Integral Limits

The outer integral limits are always h = 0 and 1. For the inner integral we need θ_{min} and θ_{max} as a function of h. The condition at $\theta = \theta_{max}$ or θ_{min} is that of Equation (6):

$$\underline{d}_{h\theta}\cdot\underline{n}_{h\theta} = \left(\underline{o} - \underline{p}_{h\theta}\right)\cdot\underline{n}_{h\theta} = 0 \quad (79)$$

As h is known, and $\underline{p}$ and $\underline{n}$ are known functions of θ, we can solve this equation to find θ:

$$\cos\theta_{\max} = \left(\frac{o_z - hH}{o_x}\right)\tan\alpha + \frac{r_h}{x_o} \quad (80)$$
$$\theta_{\min} = -\theta_{\max}$$

4.6.5 Shortest Vector

To calculate the minimum length vector to the observer from the flame surface, consider Figure 15, showing the plane y = 0. We can express the position of the observer relative to Q (the edge of the bottom disk) in terms of the two vectors $\underline{n}_{\theta=0}$ and $\underline{e}$, the flame edge vector from the bottom to the top disk:

$$\underline{o} - \underline{q} = a\underline{n}_{\theta=0} + b\underline{e} \quad (81)$$

where a and b are coefficients to be determined. Solving simultaneous equations for the x and z components yields:

$$a = \left(o_x - r_0\right)\cos\alpha - o_z\sin\alpha \quad (82)$$
$$b = \left(o_x - r_0\right)\sin\alpha + o_z\cos\alpha$$

If b is less than zero or greater than the edge length, E the shortest length vector is from the edge of the Disk 0 or Disk 1 respectively. Otherwise, there is a local minimum with h given by:

$$h_{\min} = \frac{b}{E} \qquad (83)$$

The shortest vector is then from the edge of the slice defined by h_{min}. Note also that an a coefficient in Equation (82) of less than zero means that the observer cannot view any of the flame surface so view factor for the model is zero.

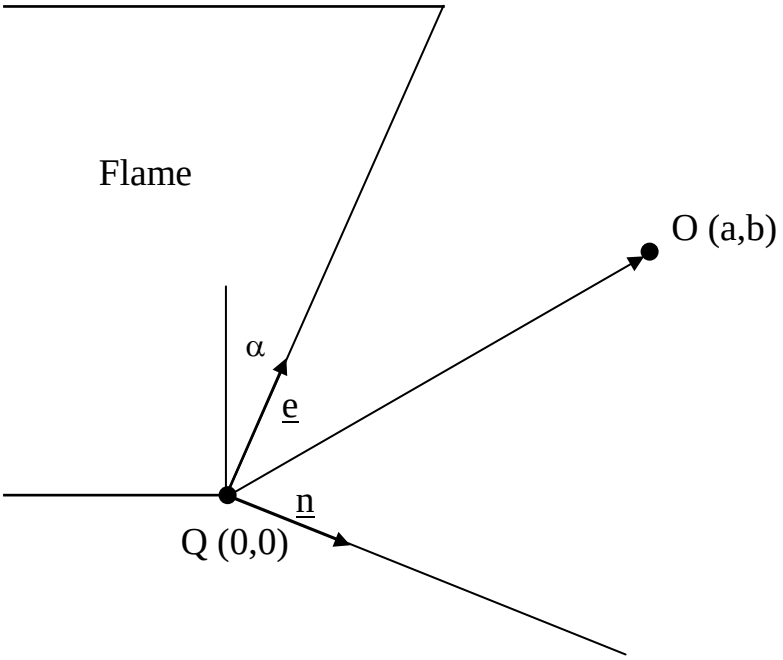

Figure 15. Determination of minimum length vector from cone surface to observer.

4.6.6 Crosswind Extent

The crosswind extent of the flame is used for the determination of whether an observer is inside or outside the flame, and for ellipse calculations. Consider a point P (position vector $\underline{p}$) on the flame boundary, then we wish to find p_Y given p_X and p_Z. But P can also be described as being on a slice through the cone defined by parametric h, where:

$$\underline{n}_D \cdot \left(\underline{p} - \underline{c}_h\right) = 0 \qquad (84)$$

$\underline{n}_D$ is the normal to the slice

This allows us to determine that h satisfies:

$$h = \frac{\left(p_X - c_{X1}\right)\sin\phi + \left(p_Z - c_{Z1}\right)\cos\phi}{\left(c_{X2} - c_{X1}\right)\sin\phi + \left(c_{Z2} - c_{Z1}\right)\cos\phi} \qquad (85)$$

The flame intersects the horizontal plane for $0 \le h \le 1$, and if it does so the crosswind extent of the flame, p_Y, is given by:

$$p_Y^2 = r_h^2 - \left|\underline{a} - \underline{c}_h\right|^2 \qquad (86)$$

5 VERIFICATION

The verification of EXPS models is summarised here. Verification has two parts. The first is against analytical solutions of the model, the second is between different models in EXPS.

The analytical solutions for point and planar observers exposed to a infinite flat planar flame are derived in Appendix B. Verification cases were designed that approximated to such a case (*i.e.* observers above and side-on to pool fires of very large radius). For observers above a pool fire (the best approximation to the analytical case, due to the lack of flame surface curvature) the results for recent PHAST releases are shown in Figure 16. Note that in all these figures, only the PHAST6.4 results use the models as described in this document.

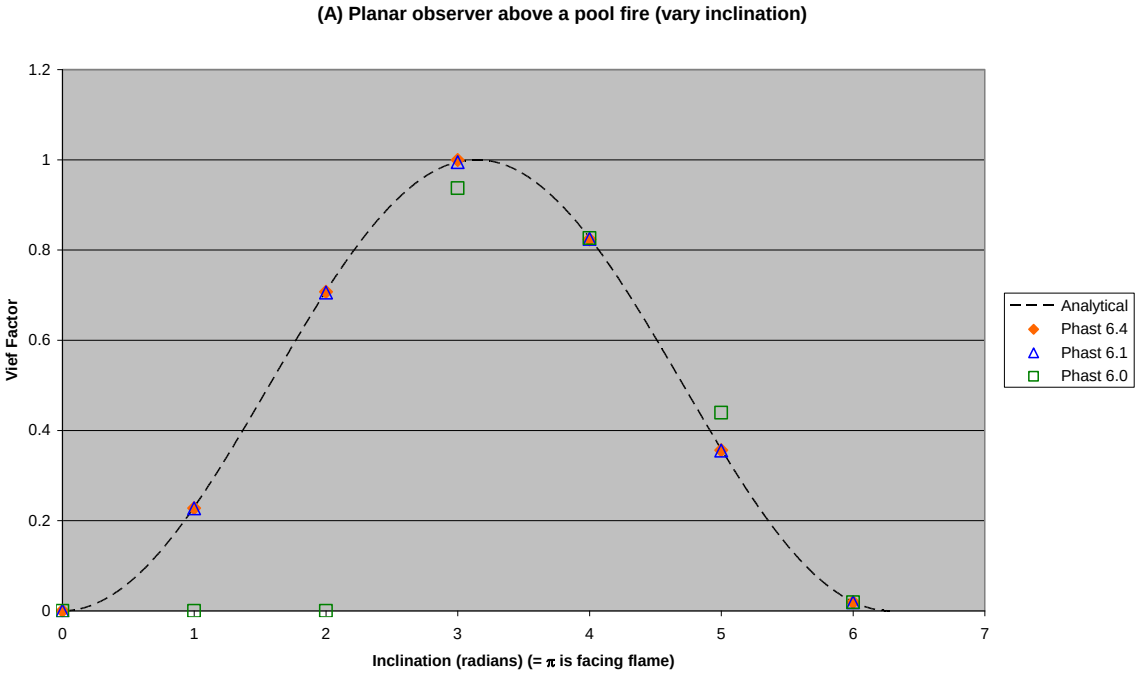

Figure 16. Planar observer above a pool fire.

For a planar observer side on to a pool fire, the approximation is not as good due to the curvature of the flame surface[17]. The results are illustrated in Figure 17. The results for PHAST 6.0 (prior to any recent quality work) are off the graph for the middle range of ζ, with a peak view factor of 7.

[17] Testing confirms increasing pool radius causes the results to approach the analytical solution ever more closely

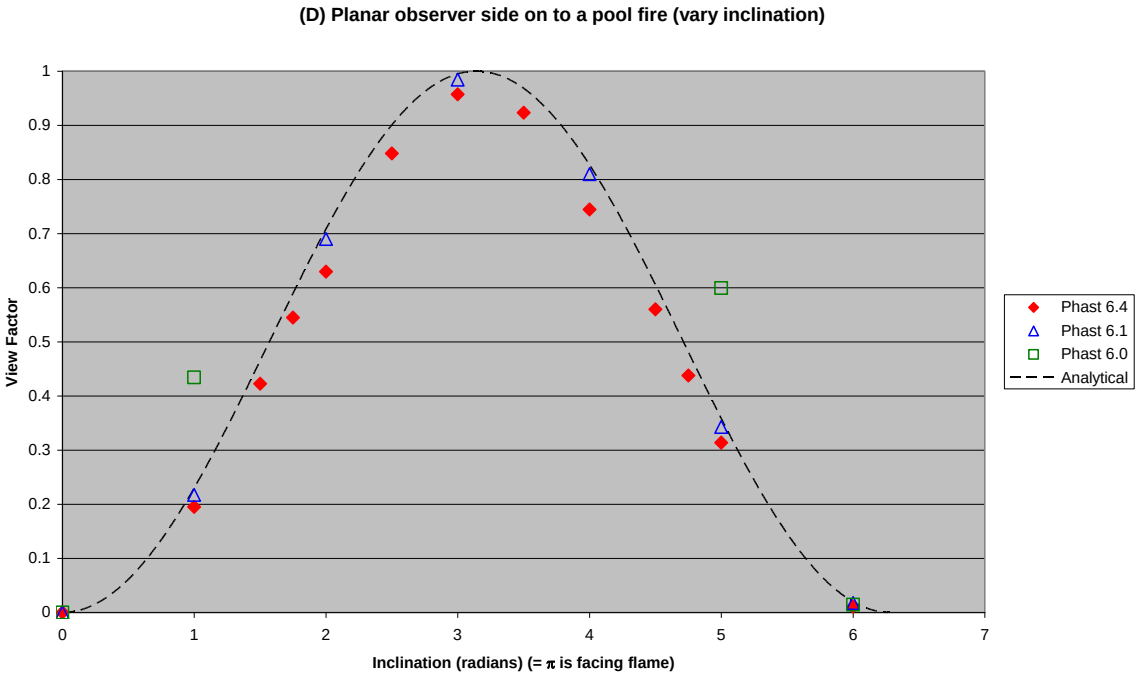

Figure 17. Planar observer side on to a pool fire

The other component of verification was comparison between the various models in this document. It was possible to set up the same flame shape using a variety of models and then compare results. The pool fire cases of Figure 16 (using the Circle model) were set up as a Frustum model case, and the cases of Figure 17 (using the cylinder model) set up using the Frustum and Cone models. Agreement between all the models was within specified tolerance.

6 FURTHER DEVELOPMENTS

Engulfed Observer

RADPNT should be rethought. A better way to test for an observer inside a flame is to first determine the intersection of the flame with the plane Y = y_{obs}. The (up to) 2 points at which each disk intersects this plane could then be determined. A frustum would then reduce to four points defining a polygon, and the MPACT_PP routine INSIDE.FOR could be used to determine if the observer was inside or outside this polygon.

The difficulty would arise where one disk did intersect the Y plane, but an adjacent one did not. In this case the intersection for the frustum would describe a triangle, the apex of which would be between disks. It may be that similar problems with current width determination would be encountered, but such cases would be more exception than rule, and overall the method would be more reliable and simpler.

Alternatively, the new methods for flame alongwind and crosswind extent could be used. These are already documented and implemented.

Alternate Parameterisation of Frustum Model

An alternate and potentially much faster method of solving the Frustum model[18] is discussed in Appendix C. It involves replacing the parameteric θ with an independent variable that better samples the arc closest to observers.

Point or Optimized BLEVEs

Additional speed increases could be achieved in these cases by using a single integral as described in 0. However, this is low priority as BLEVE is already the fastest of the flame types.

[18] Similar principles could be applied to several models, but the complex Frustum model would benefit the most.

NOMENCLATURE

Latin symbols

$\underline{a}$	Vector from disk centre to observer
$\underline{c}$	Position vector of disk centre
$\underline{d}$	Vector from flame surface to observer
$\underline{e}$	Axis (*e.g.* $\underline{e}_x$ is local x axis in terms of global co-ordinates)
E	Flame emissive power (W m^{-2}), or flame edge vector
h	Parametric frustum, cone or cylinder height (-)
I	Incident radiation (W m^{-2})
$\underline{n}$	Normal vector
r	Slice / flame radius (m)
$\underline{o}$	Position vector of observer
$\underline{p}$	Position vector of point on flame surface
P_a	Atmospheric pressure (Pa)
P_{wv}	Water vapour pressure (Pa)
r_h	Relative humidity (-)
S	Flame surface
T_a	Atmospheric temperature (K)
V	View factor
X	Absorption coefficient (-)

Greek symbols

α	Tilt of cylinder or cone edge
β_1	Angle between $\underline{d}$ and normal to flame surface
β_2	Angle between $-\underline{d}$ and observer normal
μ	Angle in plane of disk subtended by lines Y = 0 and $\underline{a}$
ϕ	Inclination of disk normal to vertical (rad)
θ	Parametric angle (rads)
τ	Atmospheric transmissivity (-)
γ	Rotation of (planar) observer about XY plane (rad)
ζ	Rotation of (planar) observer about XZ plane (rad)

Subscripts

0,1	Relating to Disk 0 or 1
x,y,z	Local co-ordinate system
X,Y,Z	Global co-ordinate system

h	Relating to specific slice in frustum, cone or cylinder defined by h
hθ	Relating to specific point on flame surface defined by h,θ
s	Projected onto the plane of a specific disk
D	Relating to a specific disk

APPENDICIES

Appendix A. Sphere Model, Point Observers

The Sphere model for point observers warrants special mention as it can be simplified even further. If the sphere centre is at the origin, then the only independent variable needed is θ, the angle between a point P on the surface and the line joining the centre and observer (taken as the X axis):

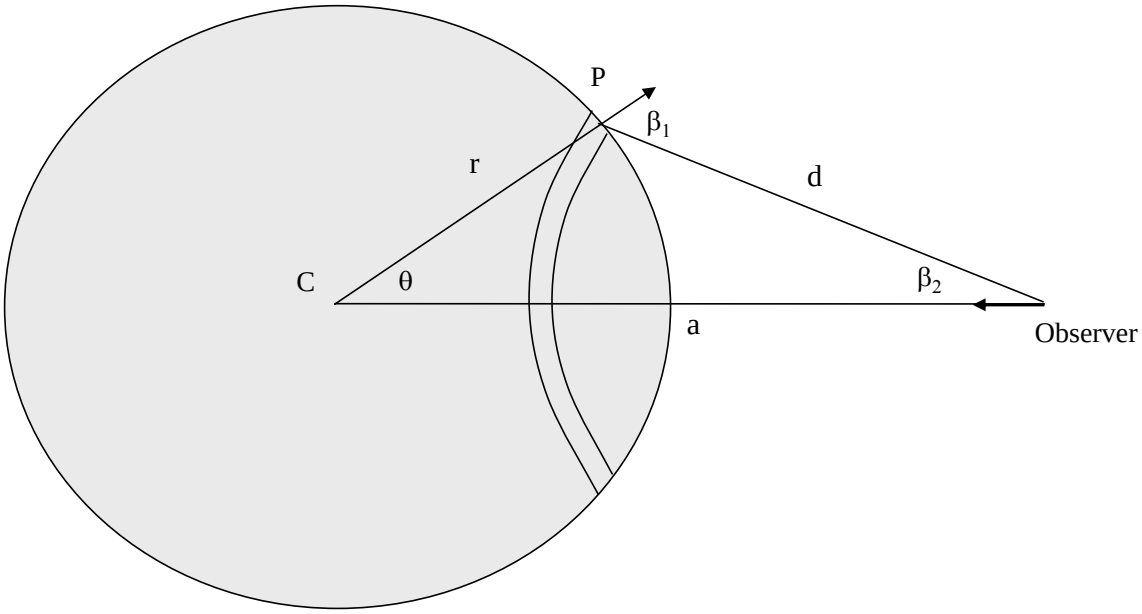

Figure 18. Sphere model for a point or optimised planar observer.

Now the surface area of the sphere defined by an increment dθ in θ is the area of the annulus shown in Figure 18. Ignoring 2nd order terms of dθ, the integral then becomes:

$$dS = 2\pi r^2 d\theta \qquad (87)$$

$$V = 2r^2 \int_0^{\cos^{-1}\left(\frac{r}{a}\right)} \frac{\tau \cos\beta_1}{\mathrm{d}^2} d\theta$$

The d^2 term is found from the cosine rule:

$$d^2 = a^2 + r^2 - 2ar\cos\theta \qquad (88)$$

And the sine rule provides β_1:

$$\sin\beta_1 = \frac{a}{d}\sin\theta \qquad (89)$$

For the case where the observer is planar but to be optimized, a similar approach may be used but with the observer normal is along the axis towards the sphere centre:

$$V = 2r^2 \int_0^{\cos^{-1}\left(\frac{r}{a}\right)} \frac{\tau}{d^2}\cos\beta_1 \cos\beta_2 d\theta \qquad (90)$$

The d^2 and cos β_1 terms are calculated as in the point observer model. The cos β_2 term is then easily determined.

Appendix B. Analytical View Factors for a Plane

Part of the verification of EXPS contrasts model results with these analytical solutions for simplified cases. These are view factor for planar and point observers adjacent to a infinite plane.

Point Observer

Consider a horizontal[19] plane (

Figure 19) with an observer at a point, O, above the centre, C, of the plane. Assuming the transmissivity, τ is constant and that the observer does not lie on a plane, the view factor, V, to the plane from the observer is

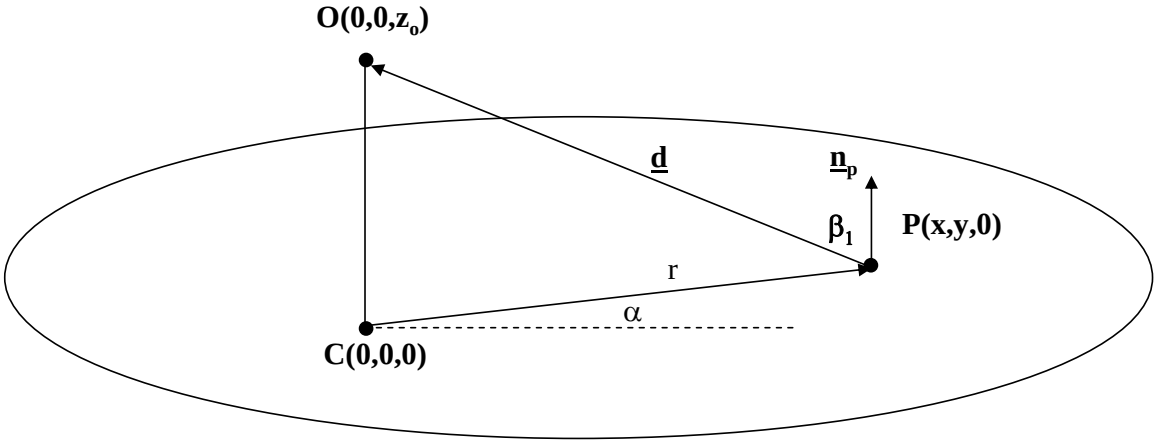

Figure 19. View factor for a point observer above a plane

$$V = \frac{\tau}{\pi} \iint \frac{\cos(\beta_1)}{d^2} dS \qquad (91)$$

Where **d** is the vector from any point P on the plane to O, and $\mathbf{n_p}$ is the unit normal vector to the plane:

$$\underline{d} = \begin{pmatrix} -r\cos\alpha \\ -r\sin\alpha \\ z_o \end{pmatrix} \qquad \underline{n}_p = \begin{pmatrix} 0 \\ 0 \\ 1 \end{pmatrix} \qquad (92)$$

Now $\cos(\beta_1)$ is related to the dot product of **d** and $\mathbf{n_p}$, so Equation (91) becomes:

$$V = \frac{\tau z_o}{\pi} \iint \frac{1}{d^3} dS \qquad (93)$$

Now for a circular area of the plane we can express the integral in terms of radius, r, from the C to P:

$$V = 2\tau z_o \int \frac{r}{d^3} dr \qquad (94)$$

Now d itself can be expressed in terms of r and z_o:

$$V = 2\tau z_o \int \frac{r}{\left(r^2 + z_o^2\right)^{3/2}} dr \qquad (95)$$

Substituting $r = s^{1/2}$ gives

[19] Note this assumes a local co-ordinate system for simplicity. The result is applicable for any plane.

$$V = \tau z_o \int \frac{1}{\left(s + z_o^2\right)^{3/2}} ds \qquad (96)$$

This is a standard integral with the solution

$$V = -\frac{2\tau z_o}{\sqrt{r^2 + z_o^2}} \qquad (97)$$

For the infinite plane, the integral limits are r = 0 and r = ∞, V is independent of z_o and evaluates to 2τ.

Plane Observer

The case where the observer lies on a plane is more complex. Consider an observer, O, located a distance z_o above the centre, C, of a horizontal (XY) source plane (Figure 20). The unit normal vector to the observer plane, $\underline{\mathbf{n}}_o$ is defined in terms of angle ω (inclination to the plane normal):

$$\underline{n}_o = \begin{pmatrix} \sin\omega \\ 0 \\ \cos\omega \end{pmatrix}, \qquad \underline{n}_p = \begin{pmatrix} 0 \\ 0 \\ 1 \end{pmatrix} \qquad (98)$$

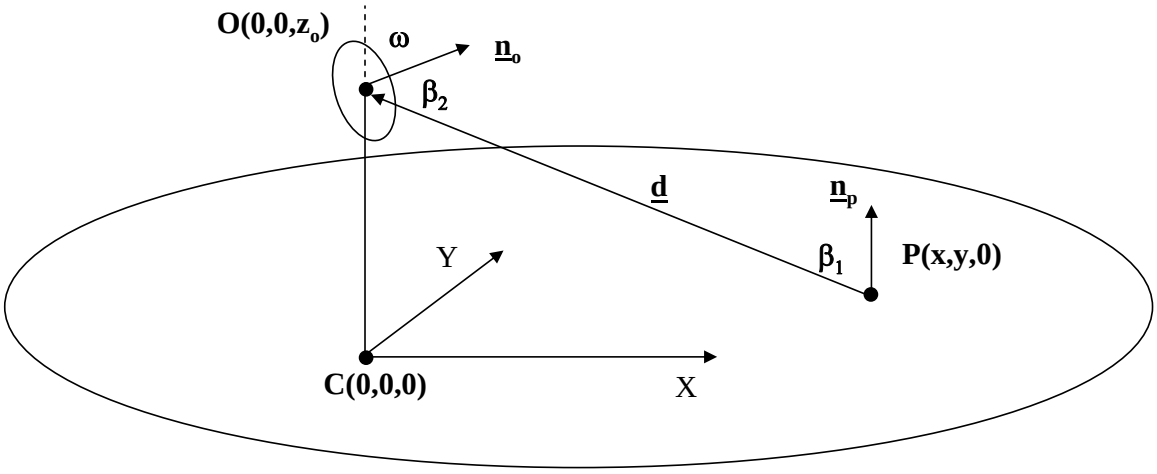

Figure 20. View factor for a planar observer above a plane

The vector **d** from a point P on the source plane to O is:

$$\underline{d} = \begin{pmatrix} -x \\ -y \\ z_o \end{pmatrix} \qquad (99)$$

Unlike for the point observer case, only part of the plane is visible (*i.e.* cos $\beta_2 > 0$) to the observer (Figure 21). By choosing the plane co-ordinate system such that y = 0 is the line along which the observer plane has maximum tilt, we ensure that the extent of the plane visible can be defined in terms of a maximum and/or minimum x value, depending on ω:

$$0 < \omega < \pi \quad \begin{cases} x_{\min} = \dfrac{z_o}{\tan\omega} \\ x_{\max} = \infty \end{cases} \qquad (100)$$

$$\pi < \omega < 2\pi \quad \begin{cases} x_{\min} = -\infty \\ x_{\max} = \dfrac{z_o}{\tan(\omega)} \end{cases}$$

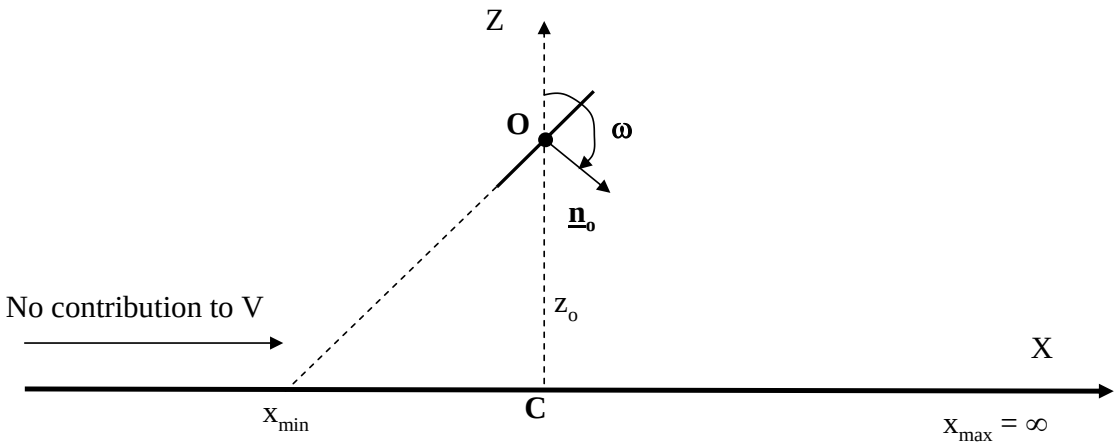

Figure 21. Partial visibility of source plane to observer
Note that when $\omega = \pi$, the integration limits are $-\infty$ to ∞, and when $\omega = 0$, the view factor is zero.

The view factor, V is calculated as:

$$V = \frac{\tau}{\pi} \iint \frac{\cos\beta_1 \cos\beta_2}{d^2} dS \qquad (101)$$

assuming that τ is constant. Replacing the cosines by dot products, and using a double integral with respect to x and y yields

$$V = \frac{\tau}{\pi} \int_{x_{min}}^{x_{max}} \int_{-\infty}^{\infty} \frac{(\underline{d} \cdot \underline{n}_p)(-\underline{d} \cdot \underline{n}_o)}{d^4} dydx \qquad (102)$$

This expands to

$$V = \frac{\tau z_o}{\pi} \int_{x_{min}}^{x_{max}} \int_{-\infty}^{\infty} \frac{x\sin\omega - z_o\cos\omega}{\left(x^2 + y^2 + z_o^2\right)^2} dydx \qquad (103)$$

The inner integral is a standard form, and evaluates between limits to give:

$$V = \frac{\tau z_o}{2} \int_{x_{min}}^{x_{max}} \frac{x\sin\omega - z_o\cos\omega}{\left(x^2 + z_o^2\right)^{\frac{3}{2}}} dx \qquad (104)$$

Expanding gives

$$V = \frac{\tau z_o}{2} \left[\sin\omega \int_{x_{min}}^{x_{max}} \frac{x}{\left(x^2 + z_o^2\right)^{\frac{3}{2}}} dx - z_o\cos\omega \int_{x_{min}}^{x_{max}} \frac{1}{\left(x^2 + z_o^2\right)^{\frac{3}{2}}} dx \right] \qquad (105)$$

These are solved by substituting $x = u^{1/2}$ is the first integral, and $x = z_o\tan(u)$ in the second to give:

$$V = -\frac{\tau}{2} \left[\frac{1}{\sqrt{x^2 + z_o^2}} \left(z_o\sin\omega + x\cos\omega\right) \right]_{x_{min}}^{x_{max}} \qquad (106)$$

For $x_{max} = \infty$, the expression inside the bracket reduces to cos ω. For x_{min}, the expression can be written as the inner product of two vectors:

$$\frac{1}{\sqrt{x_{\min}^2 + z_o^2}}\left(z_o \sin\omega + x_{\min}\cos\omega\right) = \frac{1}{\sqrt{x_{\min}^2 + z_o^2}}\begin{pmatrix} -x_{\min} \\ 0 \\ z_o \end{pmatrix} \bullet \begin{pmatrix} -\cos\omega \\ 0 \\ \sin\omega \end{pmatrix} \quad \textbf{(107)}$$

The first vector multiplied by the scalar is a unit vector, and consideration of Figure 21 illustrates that this it is the unit vector from the point X = x_{min} on the plane to the observer O. However, the second vector is identical to the first, and therefore their inner product evaluates to 1. Consequently we can simplify to:

$$V = \frac{\tau}{2}\left[1 - \cos\omega\right] \quad \textbf{(108)}$$

For the special case when $\omega = \pi$, $x_{min} = -\infty$, $x_{max} = \infty$ (*i.e.* parallel facing plane to source plane), this evaluates to τ.

Appendix C. Alternate Frustum Model

Note this model is incomplete and has not been reviewed.

Angle subtended by observer in plane of slice

In some respects the approach described for the Frustum model is unsatisfactory. If θ is the independent variable, then the arc length along the slice circumference is independent of its facing with regard to the observer. As can be seen in Figure 22, the contribution of surface segments close to θ_{max} or θ_{min} is likely to be much less than those closest to the observer. A way round this would be to use as an independent variable α, the angle subtended by the observer. The arc length δA for a given $\delta\alpha$ would then be dependent on the angle between the slice tangent and the line joining the point and the observer.

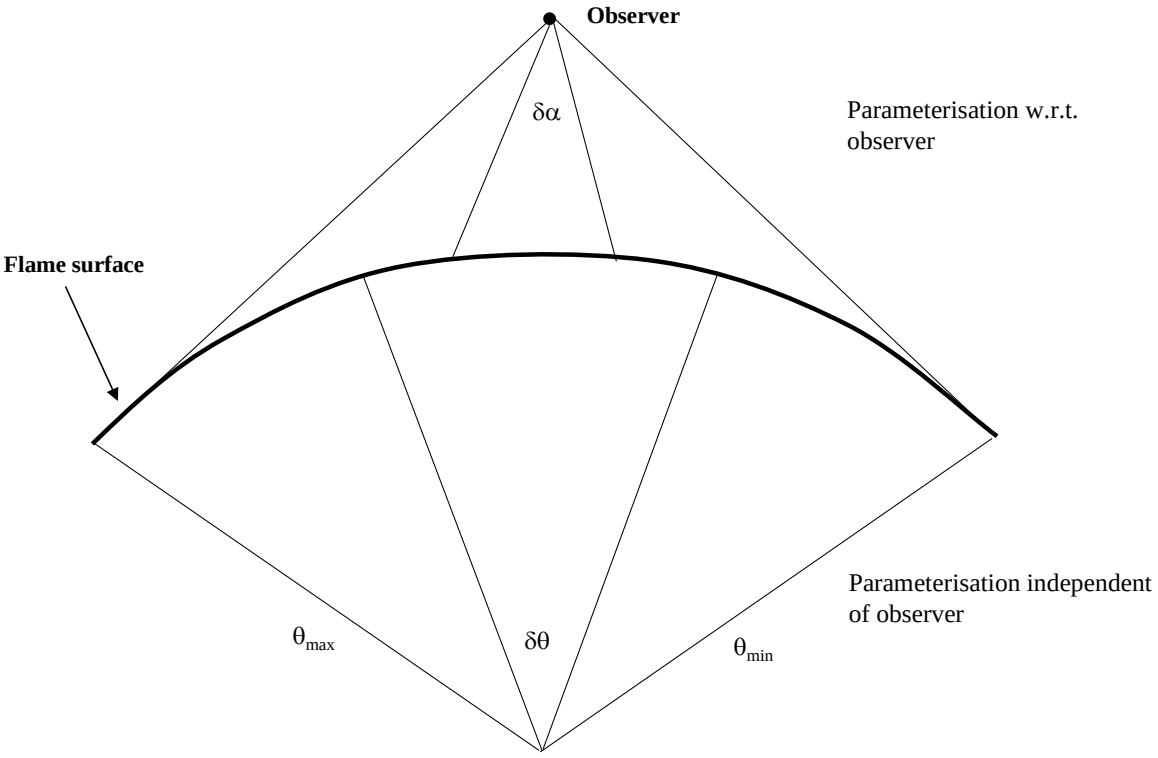

Figure 22. Alternative parameterisations of slices

The first step is straightforward: to establish a relationship between α and θ (
Figure 23). Let α be an angle in the plane of the slice between the line joining the observer and slice centre, and a point on the circumference of the slice. By the sine rule:

$$r_h \sin(\theta + \alpha) = a \sin \alpha \qquad (109)$$

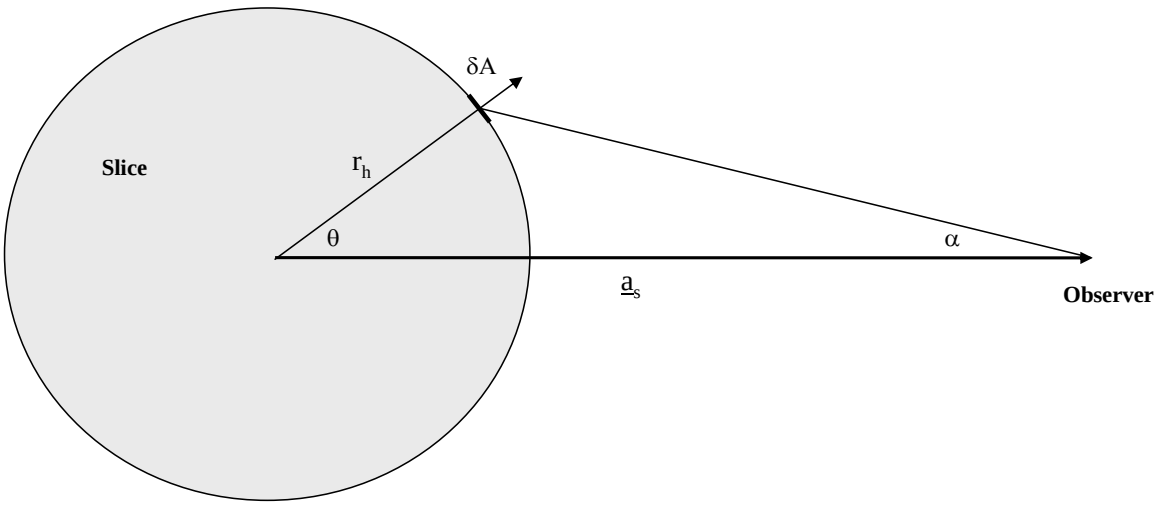

Figure 23. Arc length and angle subtended by an observer.

We must now be able to express the arc length along the slice circumference in terms of α. Differentiating the above expression, and rearranging to give arc length ($rd\theta$):

$$r_h d\theta = \left[\frac{a\cos\alpha}{\cos(\theta+\alpha)} - r_h \right] d\alpha \qquad (110)$$

The view factor integral can now be replaced by ($\theta + \alpha = \beta_1$):

$$V = \int_{h=0}^{1} \int_{\alpha_{\min}}^{\alpha_{\max}} \frac{\tau\left(\underline{\mathrm{d}} \cdot \underline{\hat{\mathrm{n}}}_{\mathrm{h}\alpha}\right)\left(-\underline{\mathrm{d}} \cdot \underline{\hat{\mathrm{n}}}_{o}\right)}{\pi\ \mathrm{d}^4} \left[\frac{\mathrm{dacos}\alpha}{\underline{\mathrm{d}} \cdot \underline{\hat{\mathrm{n}}}_{\mathrm{h}\alpha}} - \mathrm{r_h} \right] \mathrm{e}_{\alpha} d\alpha dh \qquad (111)$$

Replacement of height
A similar argument applies to the height parameter, h. For observers close in to the surface, the contribution of elements is heavily weighted towards those closest to the observer. However, for the sake of simplicity this has not been addressed. The surface does not arc away from facing the observer, and consequently the inefficiency of an even weighting will decrease rapidly as observers recede from the surface.

Point Observers
For the alternate parameterisation, the equivalent is:

$$V = \int_{h=0}^{1} \int_{\alpha_{\min}}^{\alpha_{\max}} \frac{\tau\left(\underline{\mathrm{d}} \cdot \underline{\hat{\mathrm{n}}}_{\mathrm{h}\alpha}\right)}{\pi\ \mathrm{d}^3} \left[\frac{\mathrm{dacos}\alpha}{\underline{\mathrm{d}} \cdot \underline{\hat{\mathrm{n}}}_{\mathrm{h}\alpha}} - \mathrm{r_h} \right] \mathrm{e}_{\alpha} d\alpha dh \qquad (112)$$

REFERENCES

Brzustowski, T.A., Somer, E.C., "Predicting Radiant Heating from Flares". Proceedings Division of Refining, 53, American Petroleum Institute (1973)

Cook, J., Bahrami, Z., Whitehouse, R.J., "A comprehensive program for calculation of flame radiation levels." 1st International Conference on Loss of Containment. 12-14 September, London, UK (1989)

Eisenberg N.A., Lynch C.J., Breeding R.J., "Vulnerability Model. A simulation System for Assessing Damage resulting from marine Spills." Report CG-D-136-75. Enviro Control Inc, Rockville , MD (1975)

Mudan, K. S., "Thermal Radiation Hazards from Hydrocarbon Pool Fires", Prog. Energy Combust. Sci, 10:59-80 (1984)

Raj, P.P.K., "Calculation of Thermal Radiation Hazards from LNG Fires. A Review of the State of the Art." AGA Transmission Conference (1977)

Wayne, F.D., "An economical formula for calculating atmospheric infrared transmissivities", J. Loss Prev. Process Ind. 4, pp. 86-92 (1991)

About DNV

We are the independent expert in risk management and quality assurance. Driven by our purpose, to safeguard life, property and the environment, we empower our customers and their stakeholders with facts and reliable insights so that critical decisions can be made with confidence. As a trusted voice for many of the world's most successful organizations, we use our knowledge to advance safety and performance, set industry benchmarks, and inspire and invent solutions to tackle global transformations.

Digital Solutions

DNV is a world-leading provider of digital solutions and software applications with focus on the energy, maritime and healthcare markets. Our solutions are used worldwide to manage risk and performance for wind turbines, electric grids, pipelines, processing plants, offshore structures, ships, and more. Supported by our domain knowledge and Veracity assurance platform, we enable companies to digitize and manage business critical activities in a sustainable, cost-efficient, safe and secure way.

DNV | digital@dnv.com | dnv.com/digital